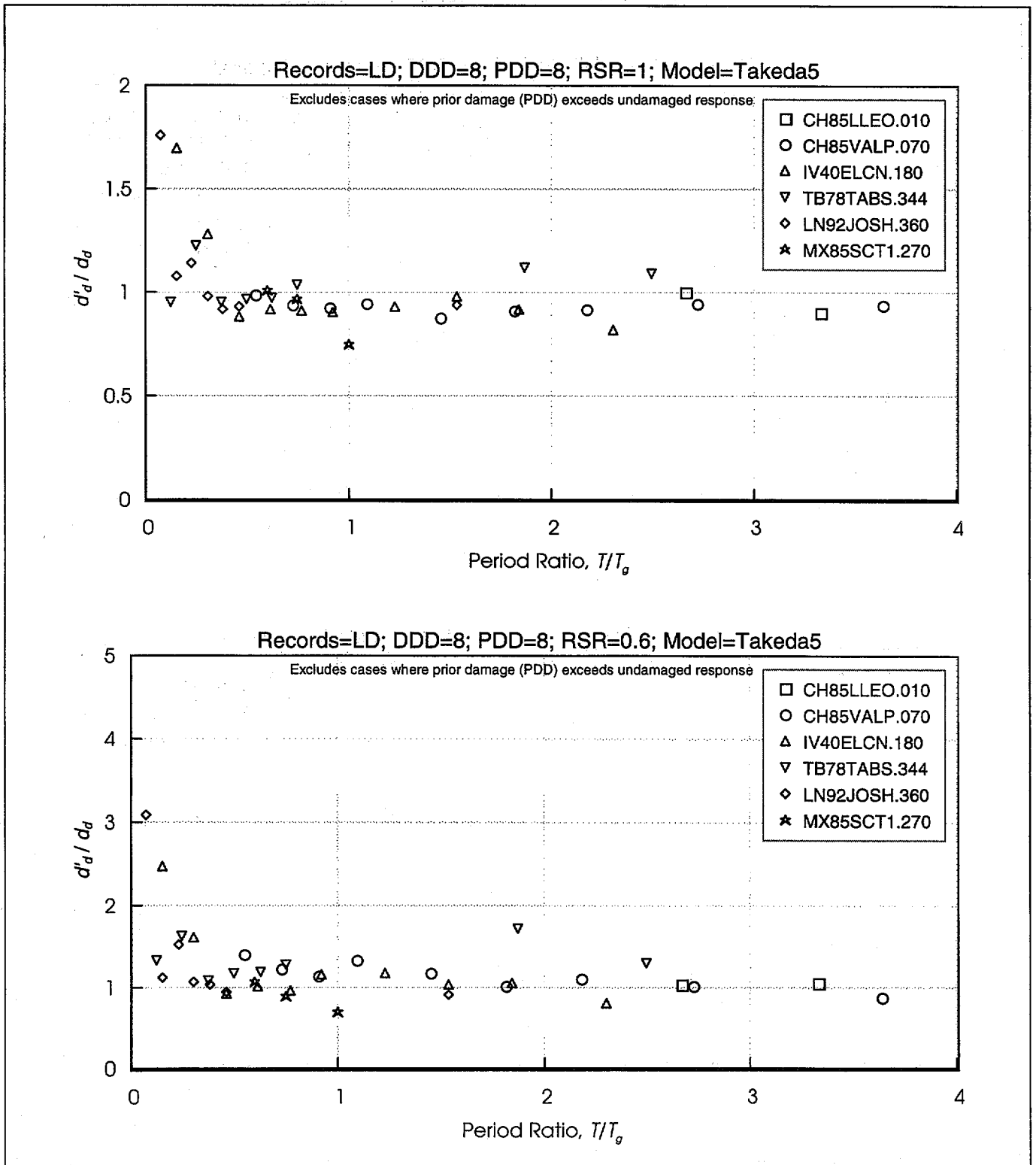
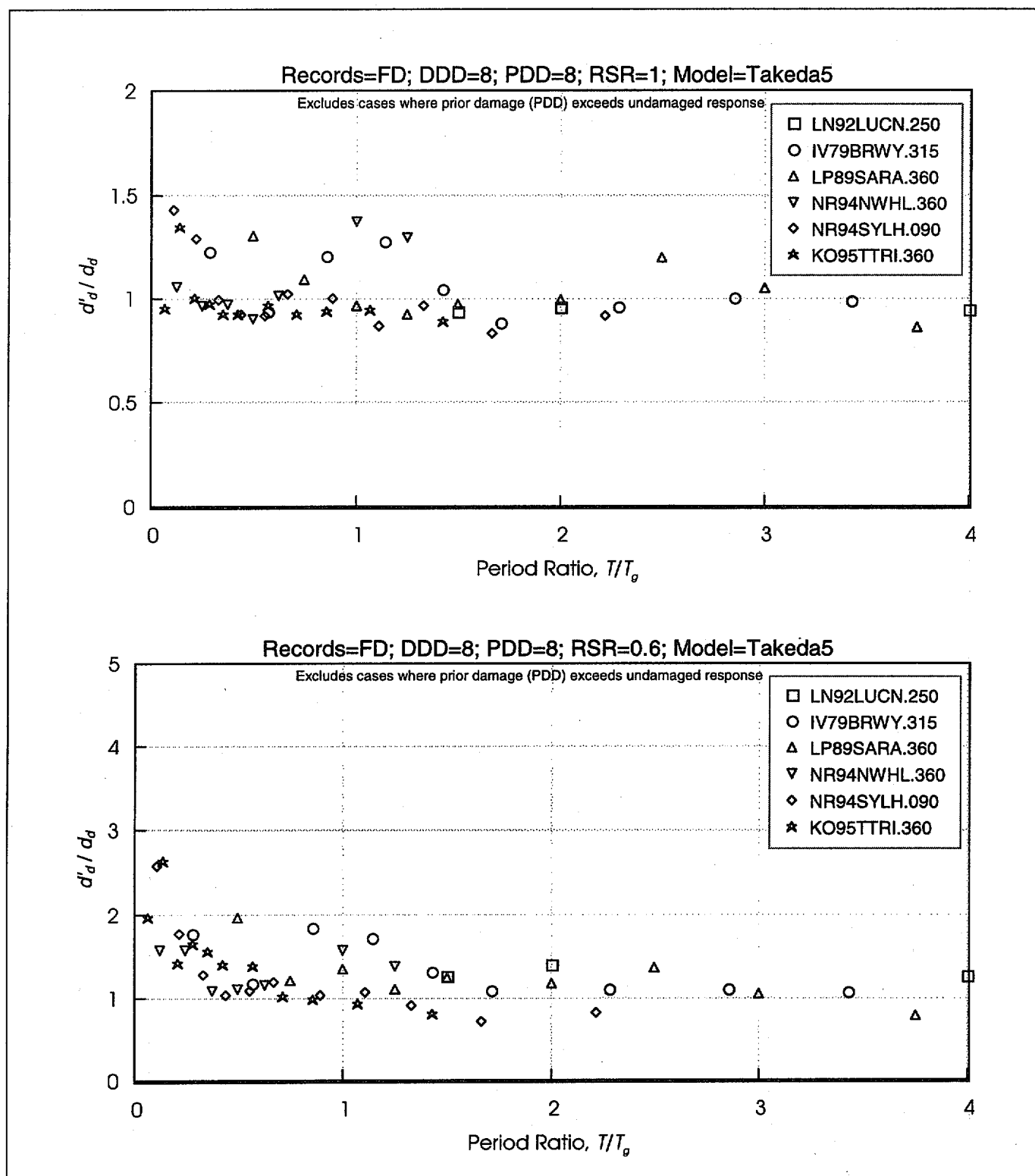


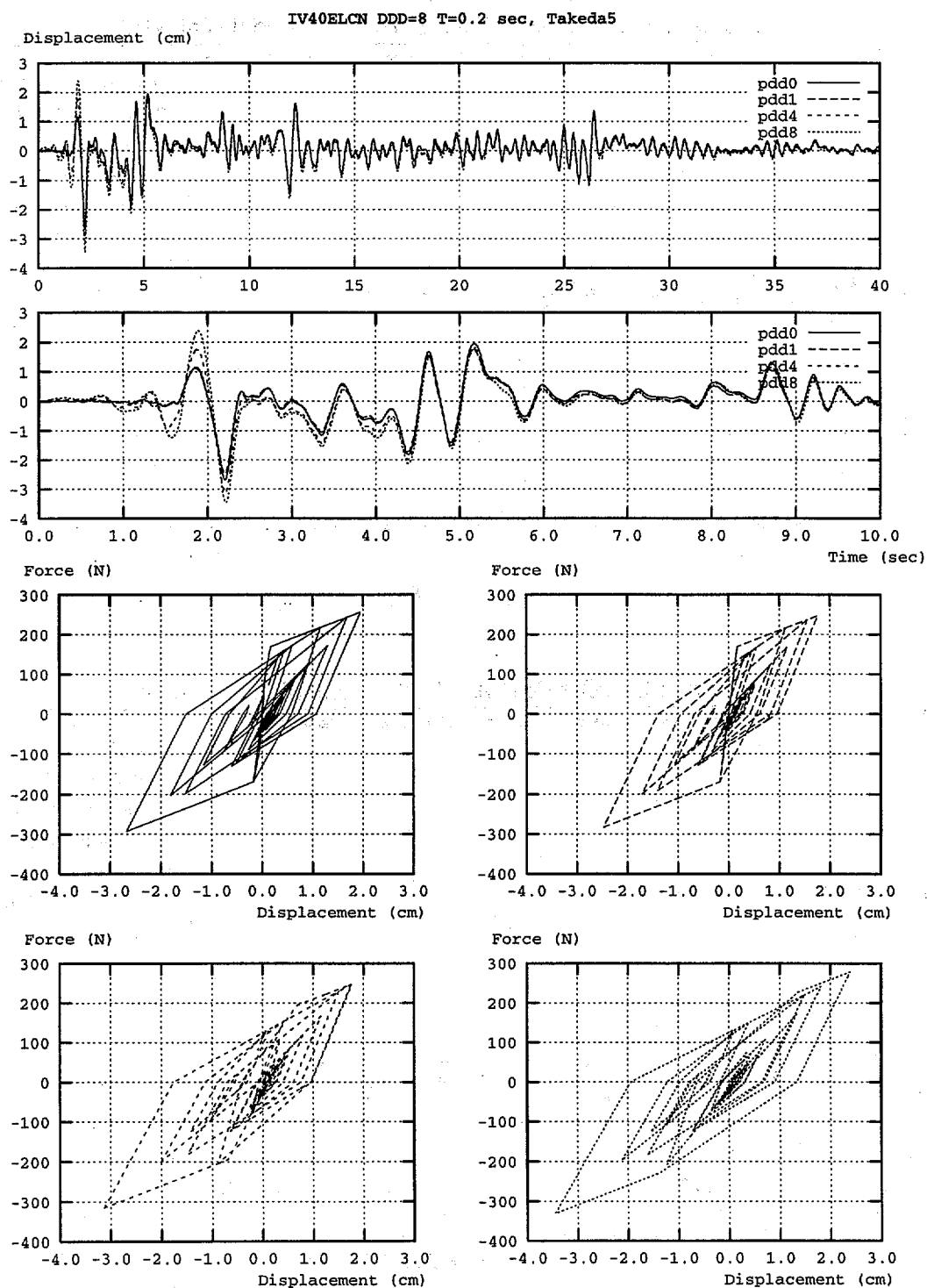
**Figure 6-38** Effect of Large Prior Ductility Demand Without and With Strength Reduction on Displacement Response of Takeda5 Models, for Short Duration Records (DDD= 8 and PDD= 8)  
DDD = Design Displacement Ductility; PDD = Prior Ductility Demand; RSR = Reduced Strength Ratio

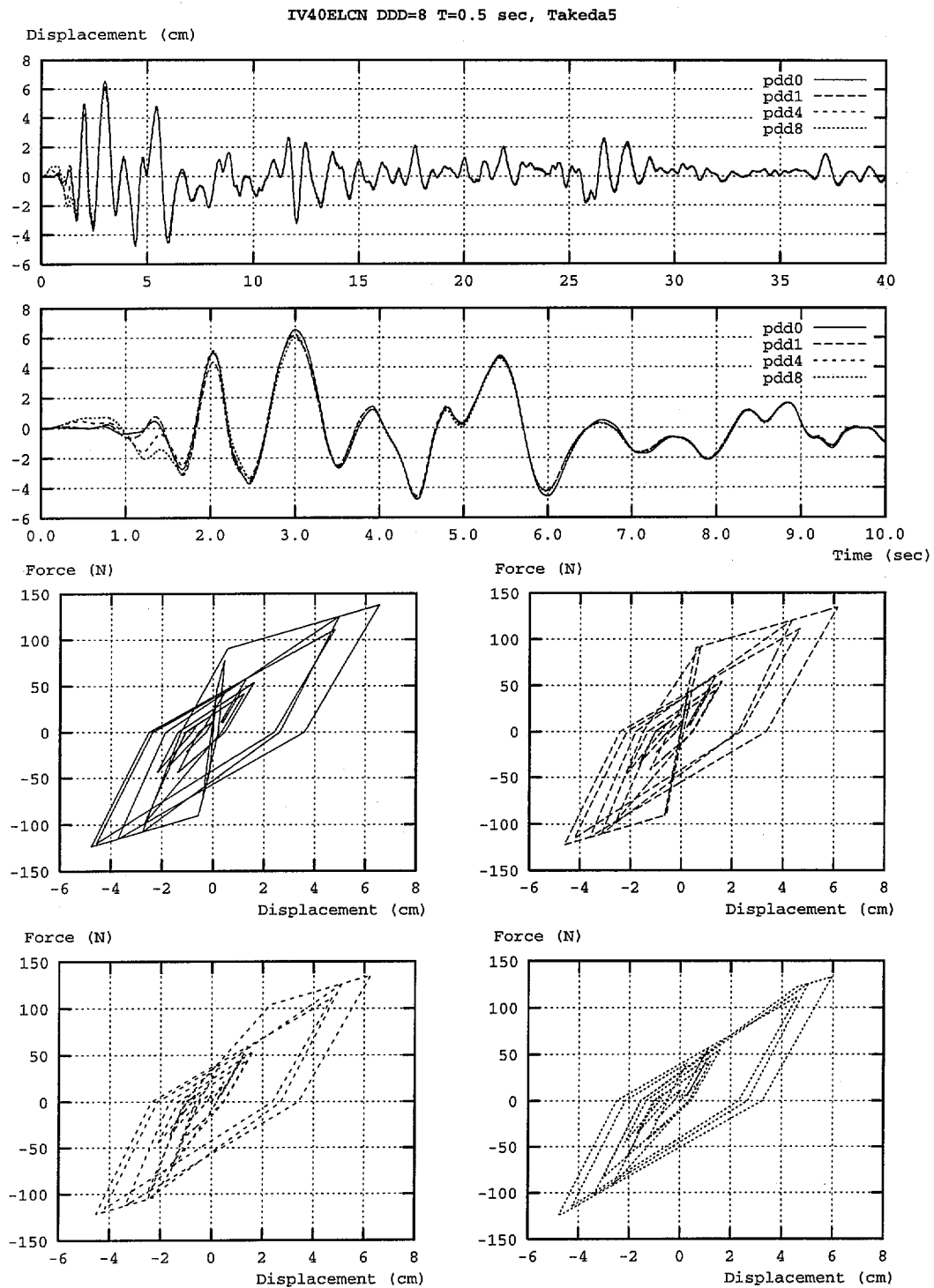


**Figure 6-39** Effect of Large Prior Ductility Demand Without and With Strength Reduction on Displacement Response of Takeda5 Models, for Long Duration Records (DDD= 8 and PDD= 8)  
 DDD = Design Displacement Ductility; PDD = Prior Ductility Demand; RSR = Reduced Strength Ratio

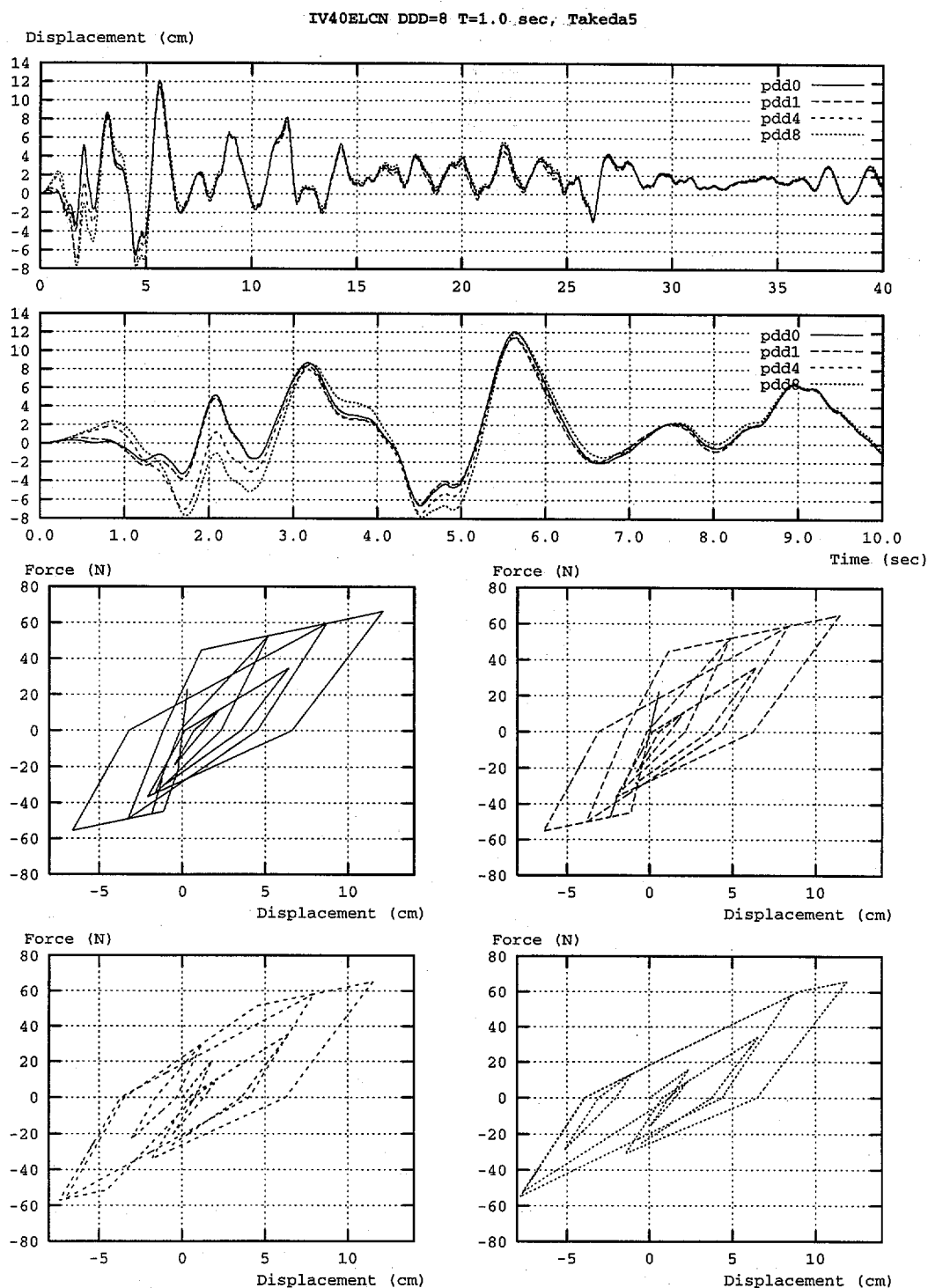


**Figure 6-40** Effect of Large Prior Ductility Demand Without and With Strength Reduction on Displacement Response of Takeda5 Models, for Forward Directive Records (DDD= 8 and PDD= 8)  
DDD = Design Displacement Ductility; PDD = Prior Ductility Demand; RSR = Reduced Strength Ratio

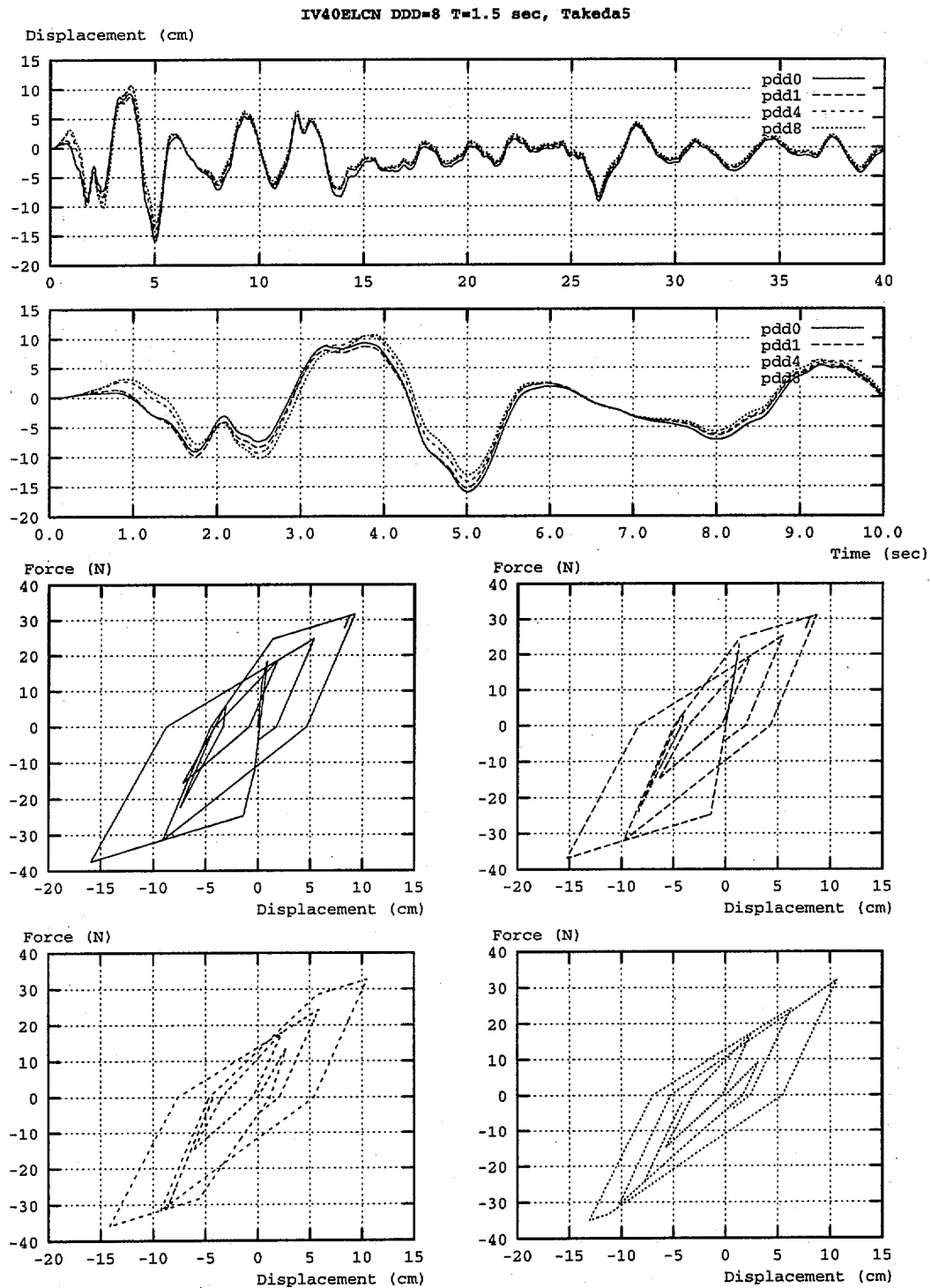




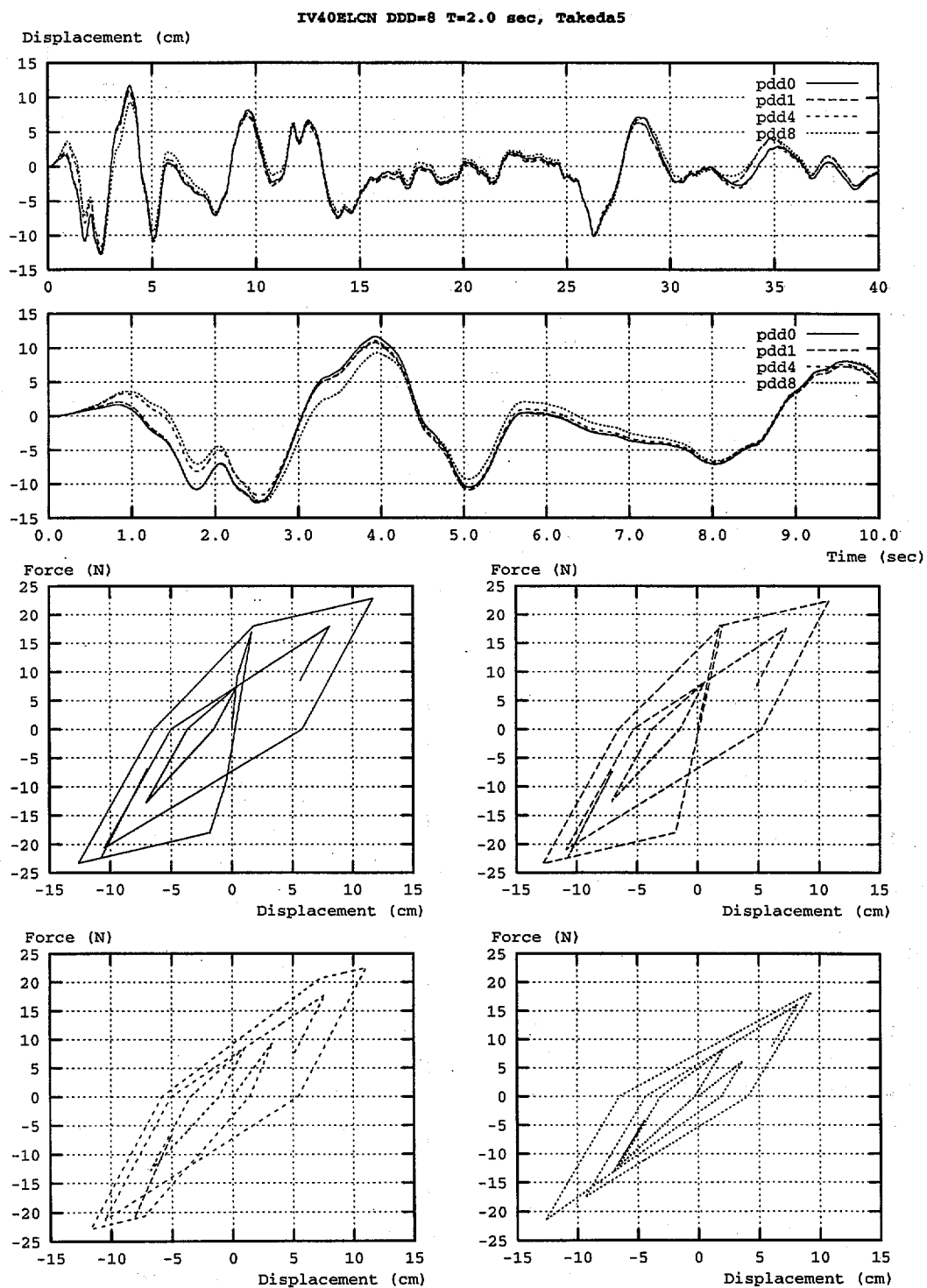
**Figure 6-42** Effect of Damage on Response to El Centro (IV40ELCN.180) for Takeda5,  $T=0.5$  sec (DDD= 8)  
 DDD = Design Displacement Ductility



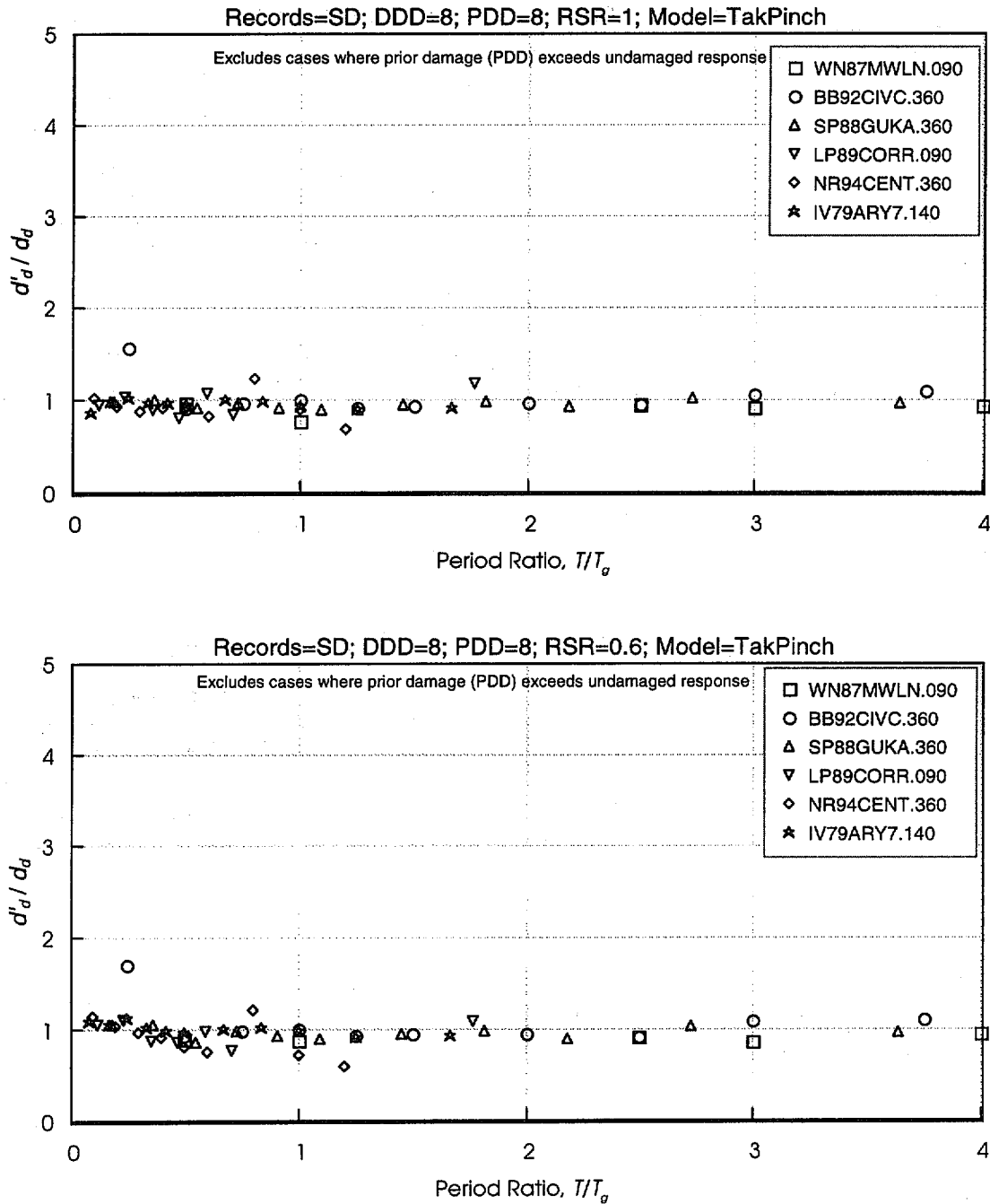
**Figure 6-43** *Effect of Damage on Response to El Centro (IV40ELCN.180) for Takeda5, T=1.0 sec (DDD= 8)  
DDD = Design Displacement Ductility*



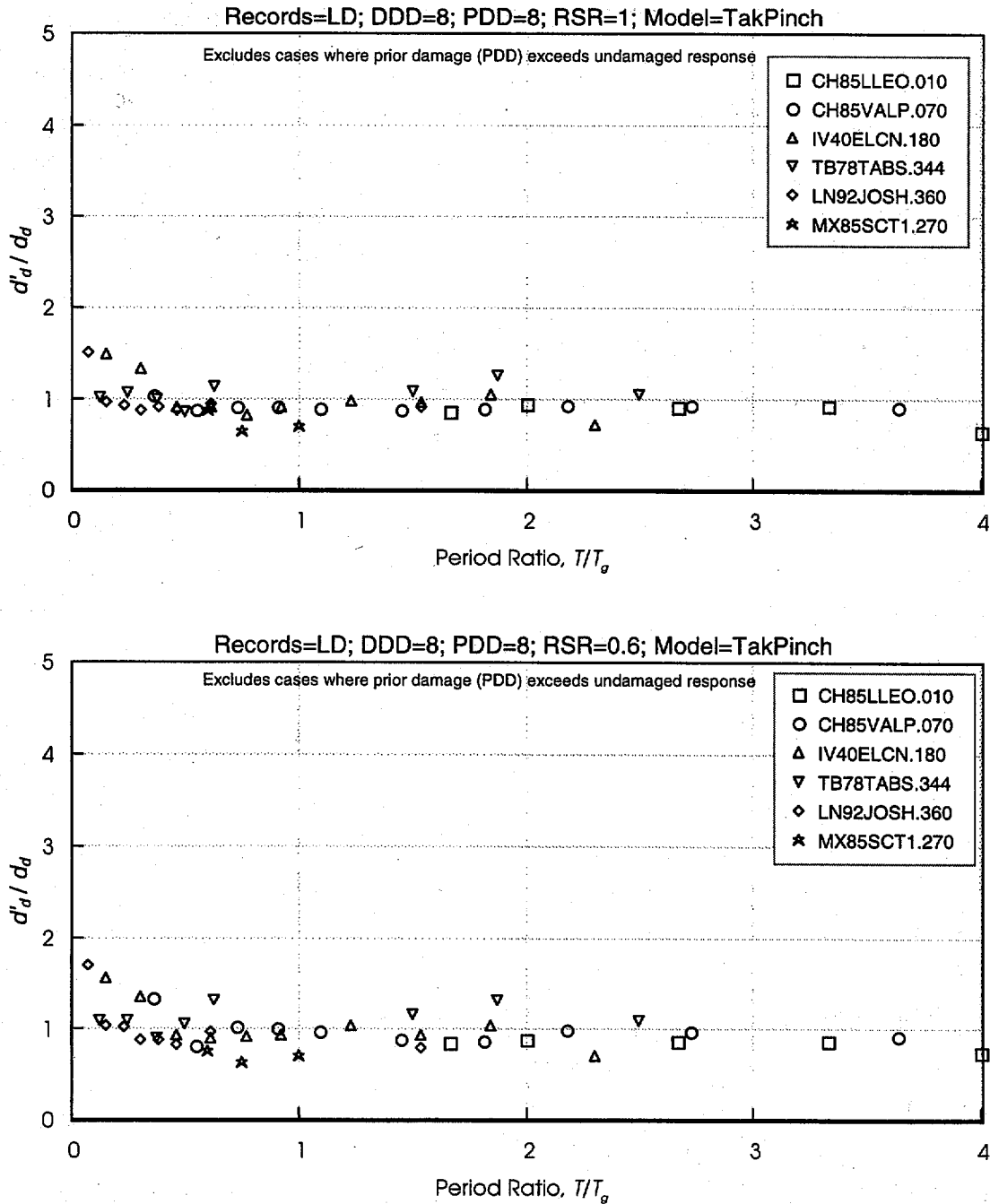
**Figure 6-44** Effect of Damage on Response to El Centro (IV40ELCN.180) for Takeda5,  $T=1.5$  sec ( $DDD= 8$ )  
**DDD = Design Displacement Ductility**



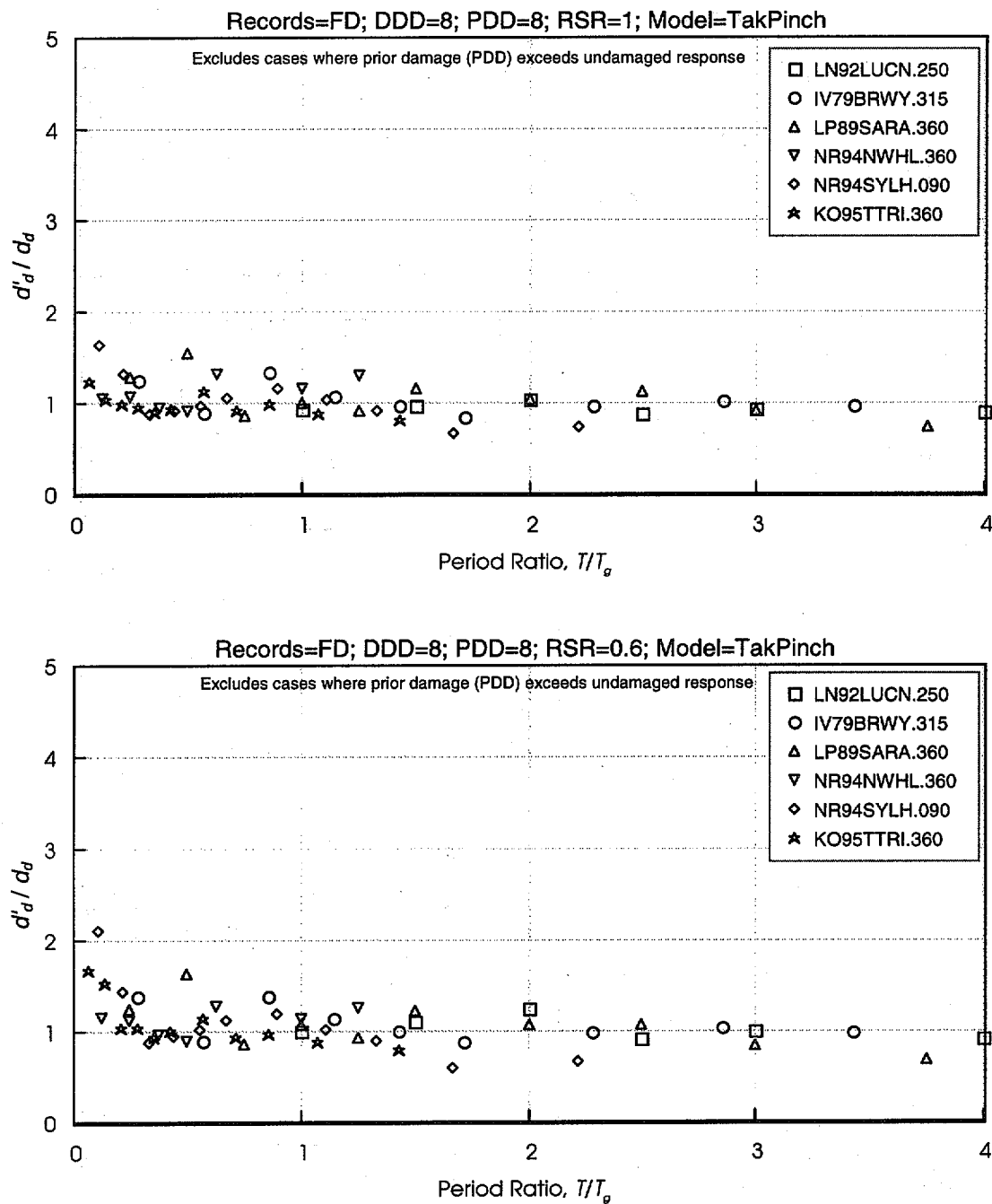




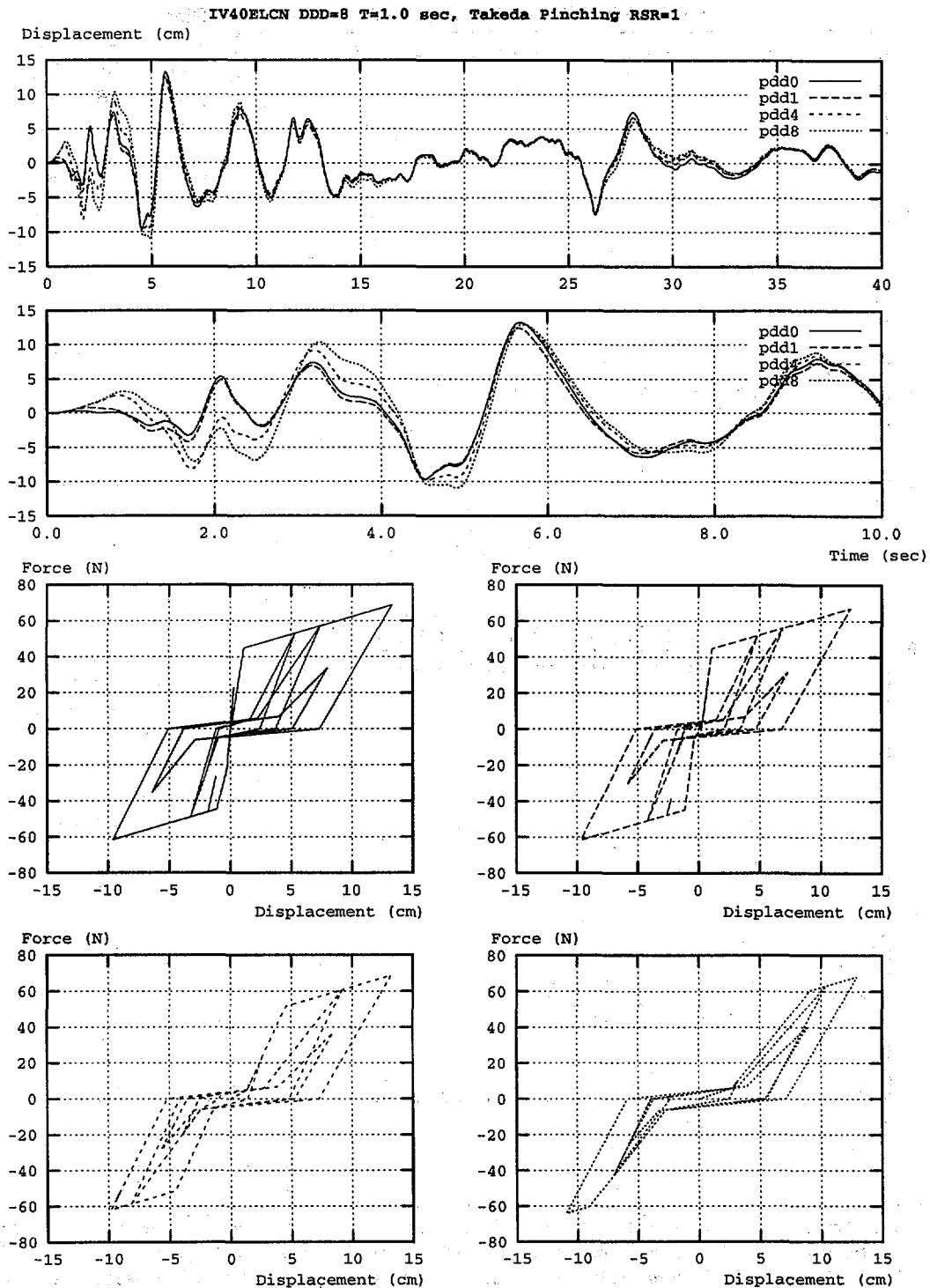
**Figure 6-46** Effect of Large Prior Ductility Demand Without and With Strength Reduction on Displacement Response of TakPinch Models, for Short Duration Records (DDD= 8 and PDD= 8)  
 DDD = Design Displacement Ductility; PDD = Prior Ductility Demand; RSR = Reduced Strength Ratio



**Figure 6-47** Effect of Large Prior Ductility Demand Without and With Strength Reduction on Displacement Response of TakPinch Models, for Long Duration Records (DDD= 8 and PDD= 8)  
DDD = Design Displacement Ductility; PDD = Prior Ductility Demand; RSR = Reduced Strength Ratio



**Figure 6-48** Effect of Large Prior Ductility Demand Without and With Strength Reduction on Displacement Response of TakPinch, for Forward Directive Records (DDD= 8 and PDD= 8)  
 DDD = Design Displacement Ductility; PDD = Prior Ductility Demand; RSR = Reduced Strength Ratio



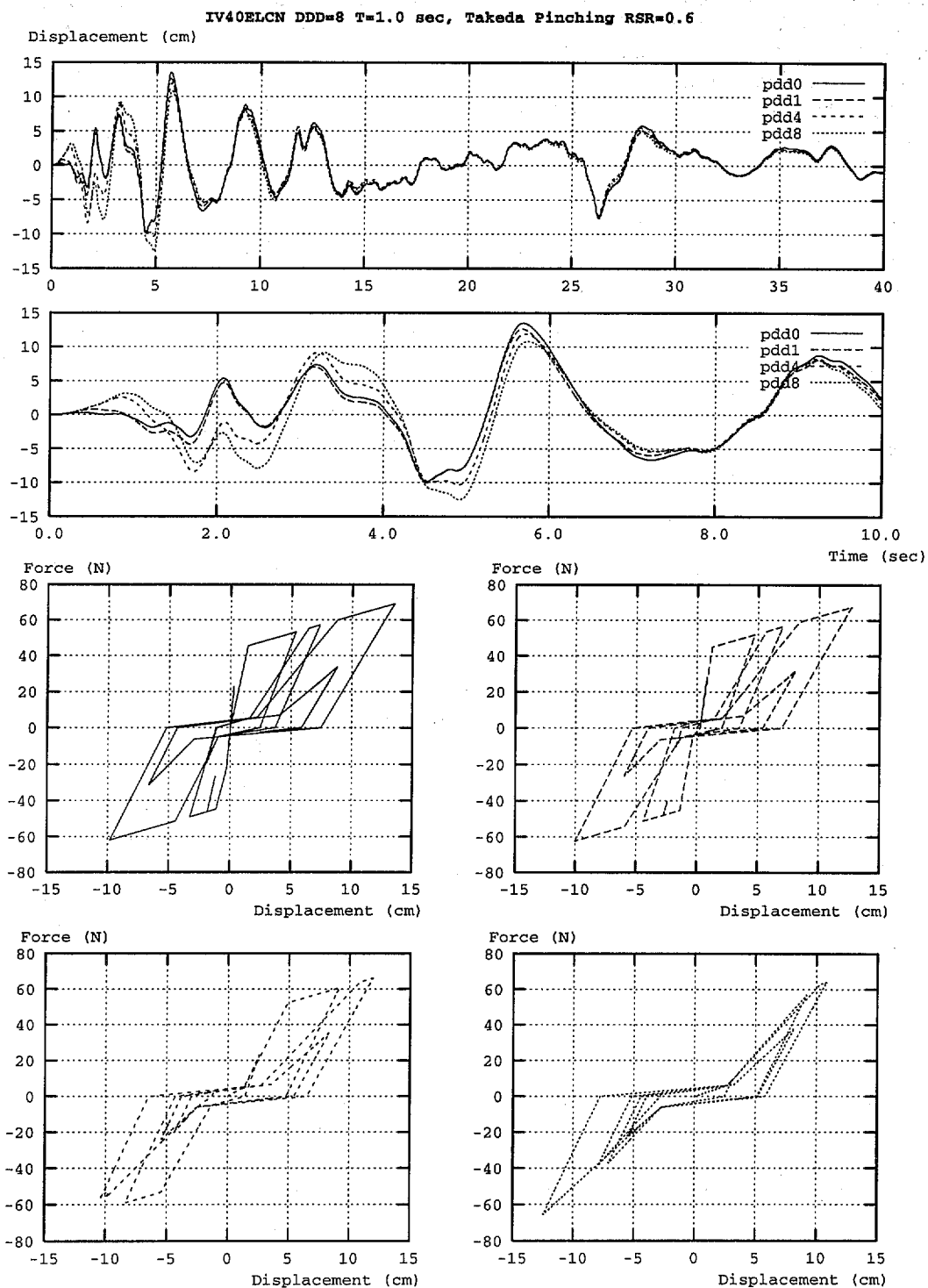


**Figure 6-50** Effect of Damage on Response of TakPinch Model to El Centro (IV40ELCN.180) for  $T=1.0$  sec and  $RSR = 0.6$  ( $DDD = 8$ )  
**DDD = Design Displacement Ductility**

ductility demand has, in general, only a small effect on displacement demand applies equally to the standard Takeda oscillator and to Takeda oscillators that exhibit pinching. The Takeda5 oscillators with initially reduced strength, given by  $RSR = 0.6$ , tended to have a response amplified to a much greater extent than is observed for the TakPinch model, reflecting the more dramatic form of strength degradation that was implemented in the Takeda5 model.

#### 6.4.3.3 Response of Takeda10 Model

The Takeda10 model is a Takeda model having post-yield stiffness equal to  $-10\%$  of the yield-point secant stiffness. As has been found previously by others, models with negative post-yield stiffness are prone to collapse, where collapse is defined as the point at which the displacement is large enough that the force resisted by the oscillator decreases to zero. Comparisons of peak displacement response are of limited value when collapse occurs. Instead, the likelihood of collapse is used to assess the impact of prior damage on response for the Takeda10 models.

Figures 6-51 to 6-53 plot the ratio,  $d'_d/d_d$ , of damaged and undamaged peak displacement response for the

Takeda10 oscillators having  $DDD = 2$ . Collapse of the damaged oscillators (whether the corresponding undamaged oscillator collapsed or not) is indicated by a ratio equal to six, and collapse of the undamaged oscillators is indicated by a ratio equal to zero. Approximately 10% of the oscillators having  $DDD = 2$  collapsed with no prior damage. This indicates that structures characterized by negative post-yield stiffnesses must remain nearly elastic if collapse is to be avoided. Prior ductility demand may cause displacement response to either increase or decrease for those oscillators that do not collapse.

Figure 6-54 plots the displacement time-history of a one-second oscillator having  $DDD = 8$  and  $PDD$  ranging from 0 (undamaged) to 8, subjected to the NS component of the 1940 El Centro record. It can be observed that prior ductility demand helps to avoid collapse in some cases, and may cause collapse in others.

#### 6.4.4 Response Statistics

Summary response statistics were prepared to identify general trends in the data.

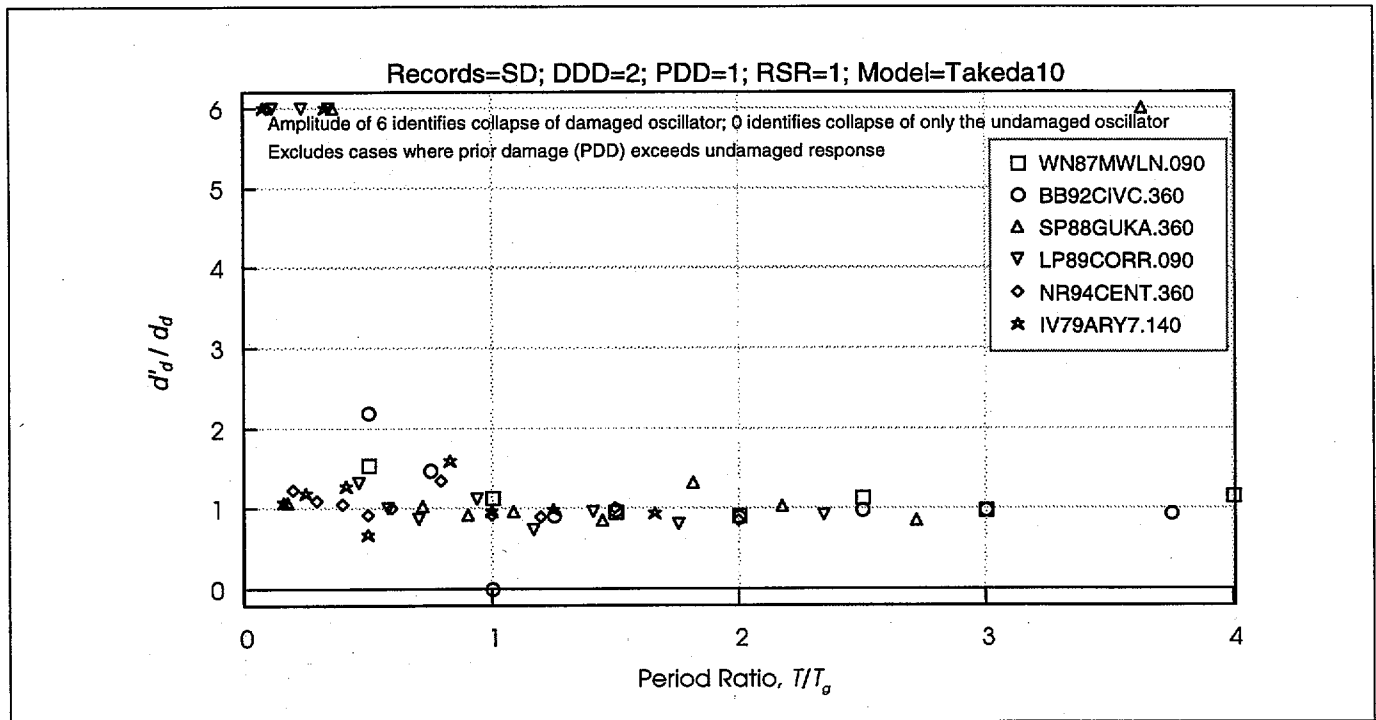


**Figure 6-51** Effect of Cracking on Displacement Response of Takeda10 Model for Short Duration Records ( $DDD = 8$  and  $PDD = 1$ )  
 $DDD$  = Design Displacement Ductility;  $PDD$  = Prior Ductility Demand;  $RSR$  = Reduced Strength Ratio

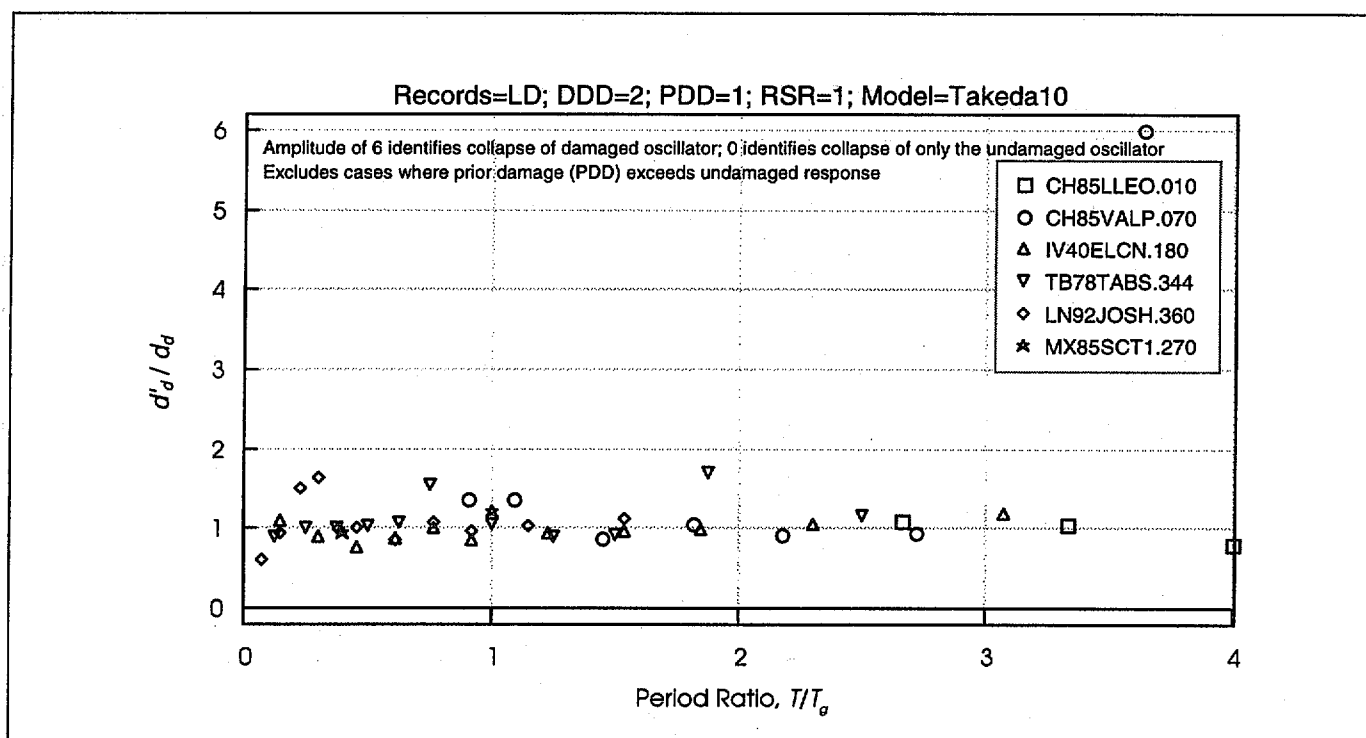


**Figure 6-52** Effect of Cracking on Displacement Response of Takeda10 Model for Long-Duration Records (DDD= 8 and PDD=1)  
DDD = Design Displacement Ductility; PDD = Prior Ductility Demand; RSR = Reduced Strength Ratio

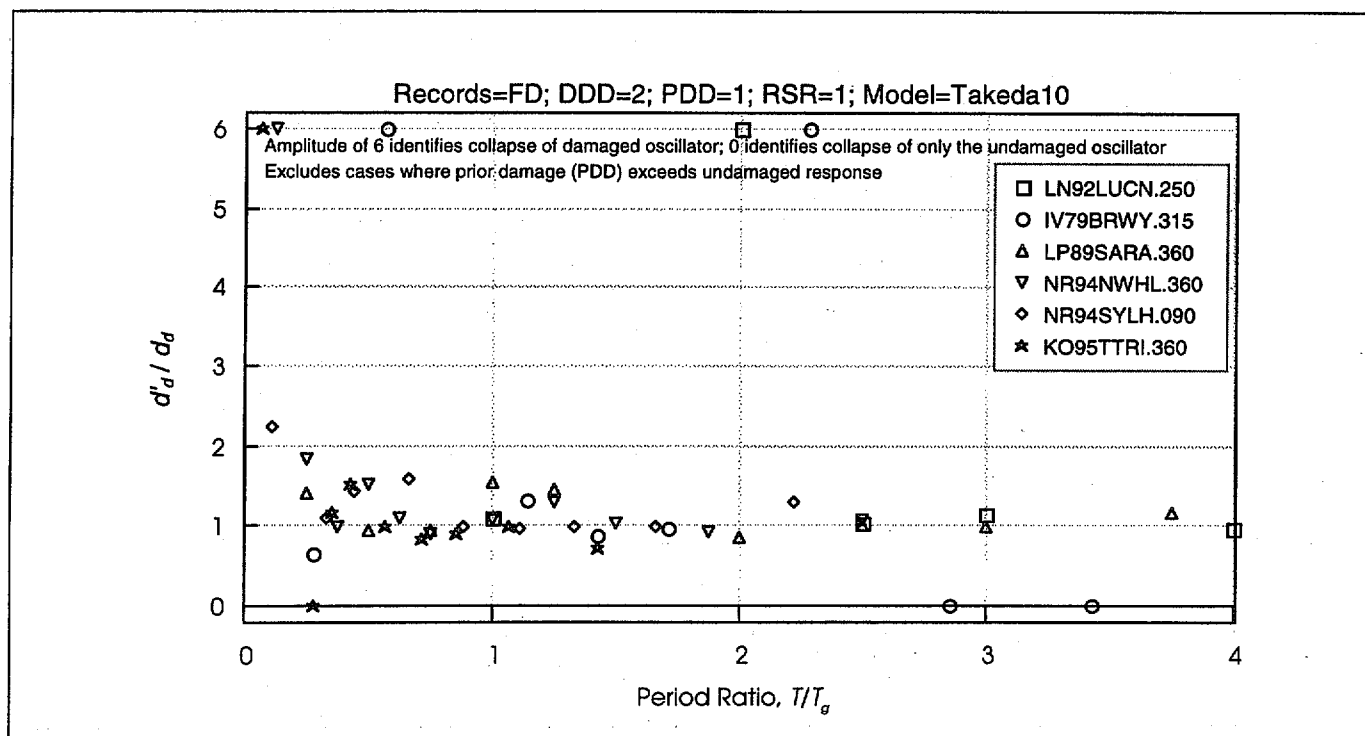


**Figure 6-53** Effect of Cracking on Displacement Response of Takeda10 Model for Forward Directive Records (DDD= 8 and PDD=1)  
DDD = Design Displacement Ductility; PDD = Prior Ductility Demand; RSR = Reduced Strength Ratio

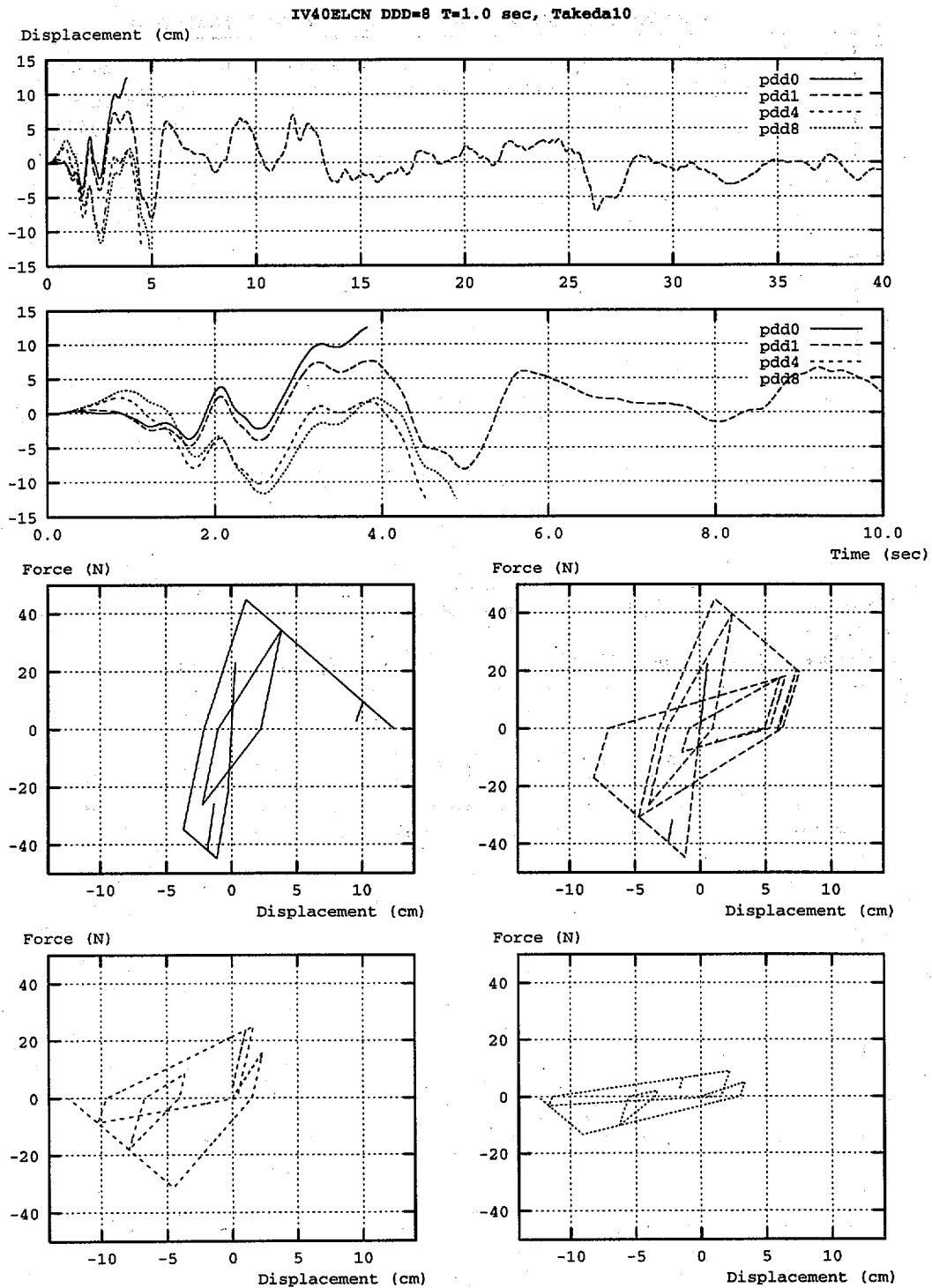


**Figure 6-54** Effect of Damage on Response of Takeda10 Model to El Centro (IV40ELCN.180) for  $T=1.0$  sec and  $RSR= 1$  (DDD= 8)  
 DDD = Design Displacement Ductility



The left side of Figure 6-55 plots mean values of the ratio of damaged and undamaged oscillator peak displacement response,  $d'_d/d_d$ , as a function of DDD and PDD, for RSR = 1, 0.8, and 0.6, for the Takeda5 model. The right side of this figure plots mean-plus-one standard deviation values of  $d'_d/d_d$ . Figure 6-56 plots similar data, but for the TakPinch model. Mean displacement ratios  $d'_d/d_d$  for the Takeda5 and TakPinch models are only slightly affected by PDD and DDD, for RSR = 1. Mean displacement ratios of the TakPinch oscillators increase slightly as RSR decreases.

strength degradation during the performance-level event. Thus, the comparison of  $d'_d$  with  $d_d$  does not provide a sufficient basis to determine the effect of strength degradation on response. Comparing response of structures having reduced strength, both with and without prior ductility demands would provide more meaningful information. Comparing data for RSR = 0.6 or 0.8, one can see in Figure 6-55 that the effect of PDD is to reduce the mean displacement ratio for Takeda5 oscillators. The capacity curve developed for a structure should incorporate strength degradation when it is anticipated.

The above discussion has focused on mean ratios of  $d'_d/d_d$ . Variability of this ratio, plotted as mean plus one standard deviation values on the right sides of Figures 6-55 and 6-56, indicates that response of a

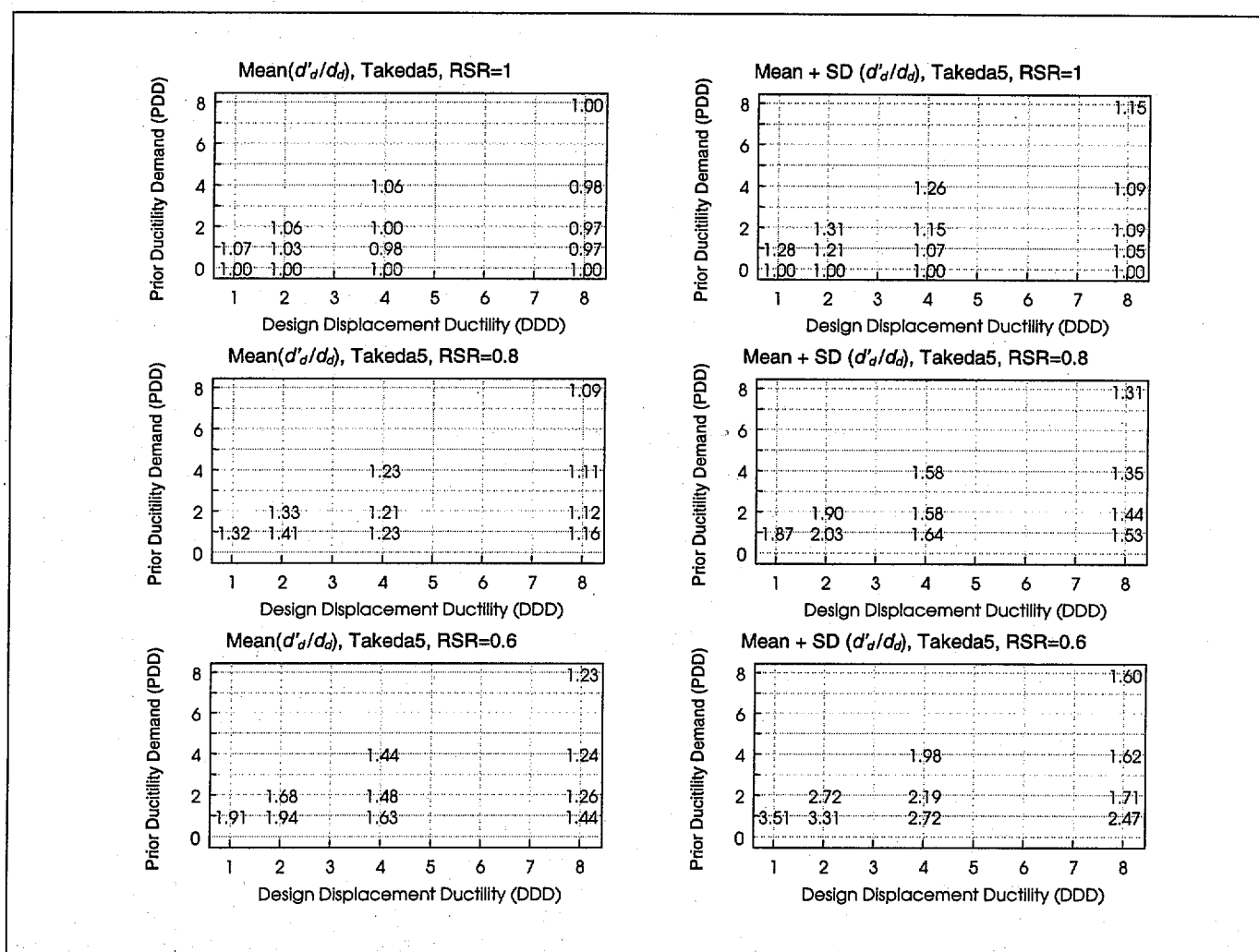


Figure 6-55 Mean and Standard Deviation Values of  $d'_d/d_d$  for Takeda5 Model.

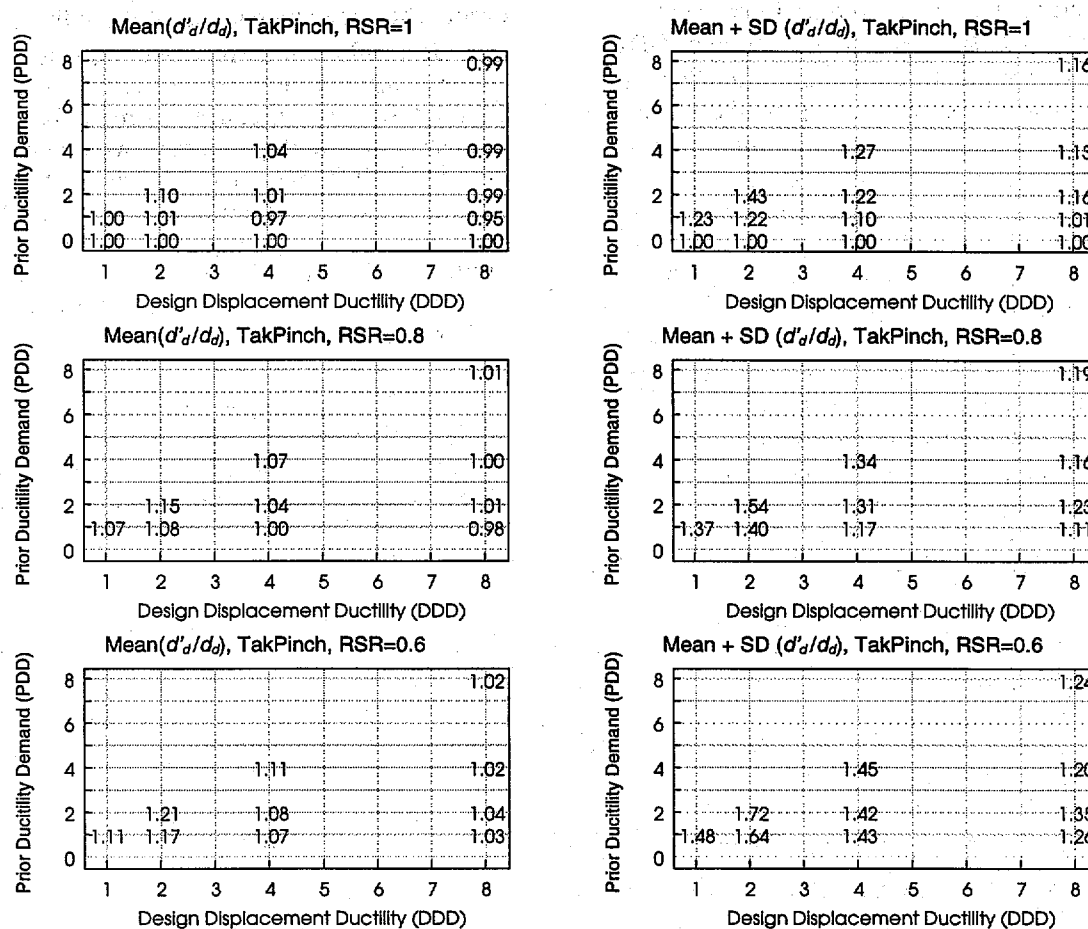


Figure 6-56 Mean and Standard Deviation Values of  $d'_d/d_d$  for TakPinch Model.

damaged structure to a given earthquake varies relative to the response in the initially-undamaged state. However, this variability is insignificant in the context of variability arising from other sources. For example, the hysteresis model and earthquake ground motion have a greater effect on response displacements than the variability arising due to prior damage. Figures 6-32 to 6-34 indicate how different the peak displacement response of undamaged Takeda and bilinear models can be to a given earthquake.

Figure 6-57 shows the percentage of Takeda10 oscillators that reached their collapse displacement. It can be observed that 10% or more of those structures designed to achieve a displacement ductility of two collapsed. This indicates the need to ensure that structures having negative post-yield stiffnesses remain nearly elastic if collapse is to be avoided. Strength

reduction tends to increase the tendency of the oscillators to collapse. No clear trend emerges as to the effect of PDD on the tendency of these oscillators to collapse.

## 6.5 Nonlinear Static Procedures

### 6.5.1 Introduction

Nonlinear static analysis is used to estimate inelastic response quantities without undertaking the effort required for inelastic dynamic analyses. Several methods are presently in use. No consensus has emerged as to the applicability and relative accuracy of the methods, which are collectively known as nonlinear static procedures (NSP). These procedures each focus

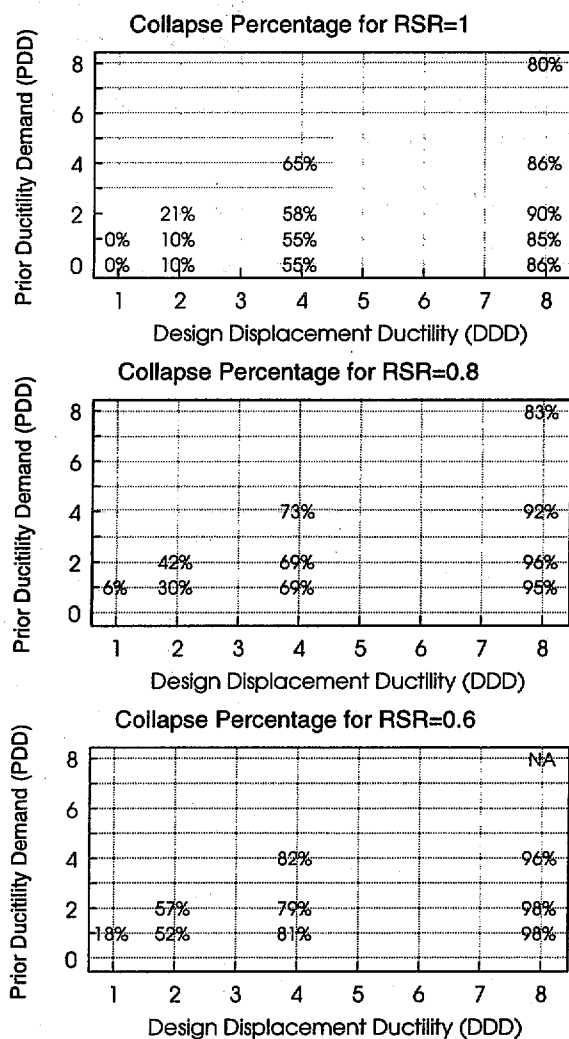


**Figure 6-57** Percent of Takeda10 Oscillators that Collapsed

on different parameters for determining estimates of peak displacement response. Consequently, NSP displacement estimates may be affected to different degrees by differences in hysteretic model, initial stiffness, lateral strength, and post-yield stiffness.

Section 6.5.2 describes three nonlinear static methods; displacement coefficient, secant, and capacity spectrum methods. Differences among the methods and the implications for estimating displacements are discussed in Section 6.5.3. Assumptions made to extend the methods to cases with prior damage are discussed in Section 6.5.4. Displacement estimates obtained using

NSP are compared with values computed from dynamic analyses in Section 6.6.

### 6.5.2 Description of Nonlinear Static Procedures

The methods are briefly described in this section for cases assumed to correspond most closely to the dynamic analysis framework of Section 6.3.3, representing wall buildings at the collapse prevention performance level. The reader is referred to FEMA 273 for greater detail on the displacement coefficient method, and to ATC-40 for greater detail on the secant and capacity spectrum methods. The displacement

coefficient method described here is the same as in FEMA 273.

### 6.5.2.1 Displacement Coefficient Method

The displacement coefficient method estimates peak inelastic displacement response as the product of a series of coefficients and the elastic spectral displacement. The peak displacement estimate,  $d_d$ , is given by

$$d_d = C_0 C_1 C_2 C_3 S_a \left( \frac{T_e}{2\pi} \right)^2 \quad (6-2)$$

where coefficients  $C_0$  through  $C_3$  modify the spectral displacement, given by the product of the elastic spectral acceleration,  $S_a$ , and  $(T_e/2\pi)^2$ , where  $T_e$  is an effective period based on the effective stiffness determined using the construction of Figure 6-58. In the above,  $C_0$  relates the spectral displacement and the expected roof displacement, and is set at 1 for SDOF systems. The coefficient  $C_1$  accounts for the amplification of peak displacement for short-period systems, is set at 1 for  $T_e > T_g$ , and is computed as follows for  $T_e < T_g$ :

$$C_1 = \frac{1}{R} + \left( 1 - \frac{1}{R} \right) \frac{T_g}{T_e} \quad (6-3)$$

where  $R$  = the strength-reduction factor, given by the ratio of the elastic base shear force and the effective

yield strength,  $F_{ye}$ , illustrated in Figure 6-58. An optional limit of 2 on  $C_1$  was not applied in the analyses described here.

The coefficient  $C_2$  accounts for the type of hysteretic response. At the collapse prevention performance level,  $C_2$  varies linearly between 1.5 at 0.1 sec and 1.2 at  $T_g$ , and remains at 1.2 for  $T_e$  greater than  $T_g$ .

The coefficient  $C_3$  accounts for increases in displacements that arise when  $P-\Delta$  effects are significant. Because the dynamic analyses did not include second-order effects,  $C_3$  was assigned a value of 1. However, the Takeda 10 models had a negative post-yield stiffness of 10 percent, which approximates  $P-\Delta$  effects

### 6.5.2.2 Secant Method

The secant method assumes that the peak displacement response of a nonlinear system can be estimated as the peak response of an elastic system having increased period. An idealized lateral-force/displacement curve for the structure is developed using a static "pushover" analysis. The elastic response of the structure is computed using a response-spectrum analysis, using initial component stiffness values. The resulting elastic displacements are used to obtain revised stiffness values for the components, set equal to the secant stiffness defined at the intersections of the component force/displacement curves and the elastic displacements obtained from the response-spectrum analysis. Using these revised stiffness values, another response-spectrum analysis is performed, and iterations continue

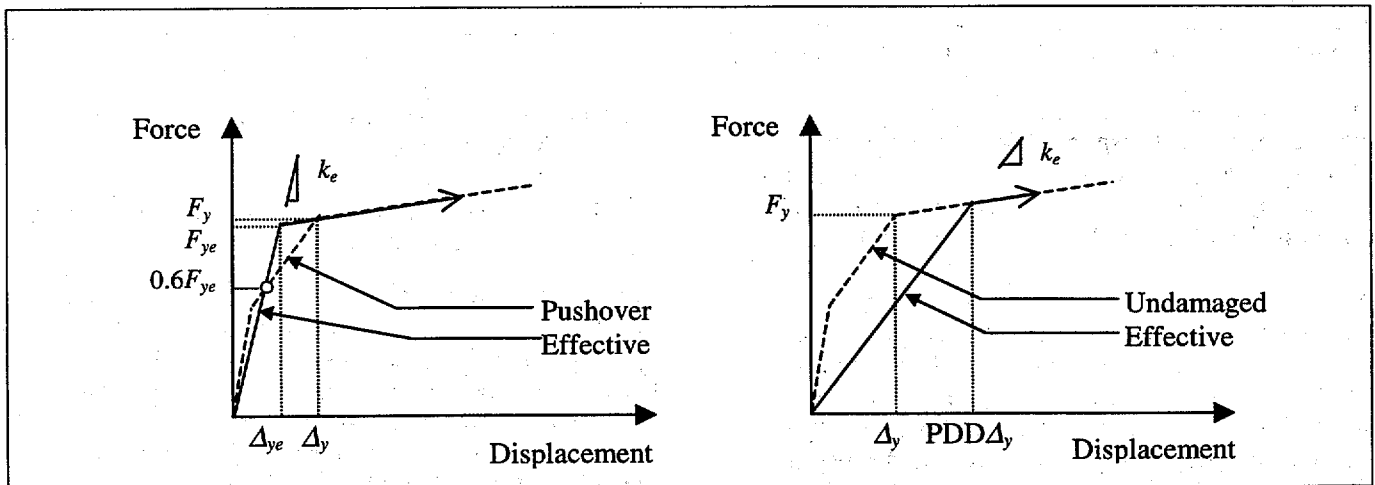


Figure 6-58 Construction of Effective Stiffness for use with the Displacement Coefficient Method

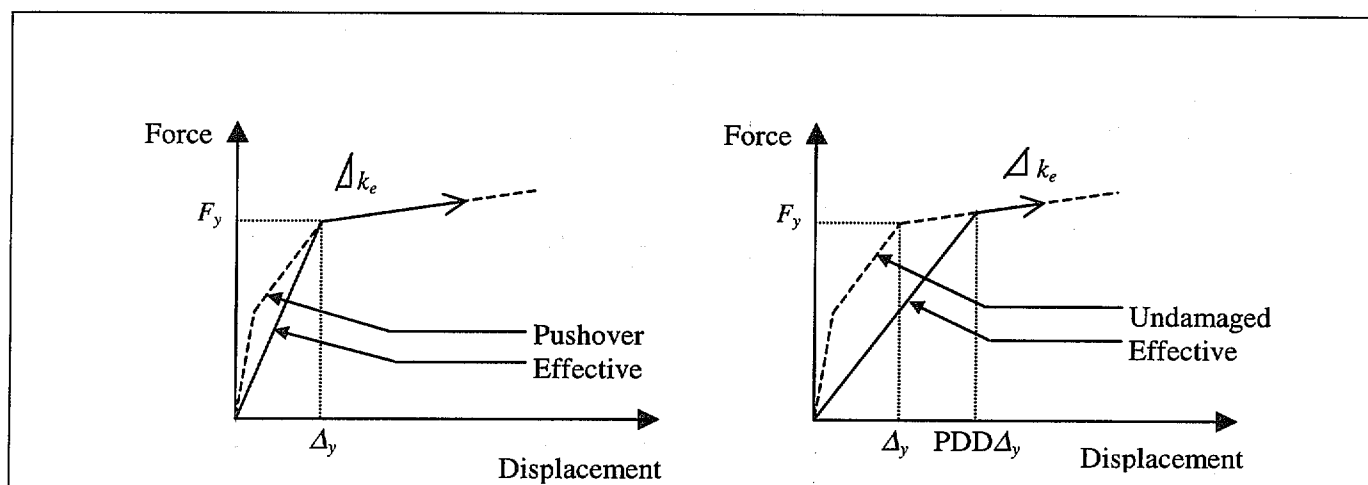


Figure 6-59 Initial Effective Stiffness and Capacity Curves Used in the Secant and Capacity Spectrum Methods

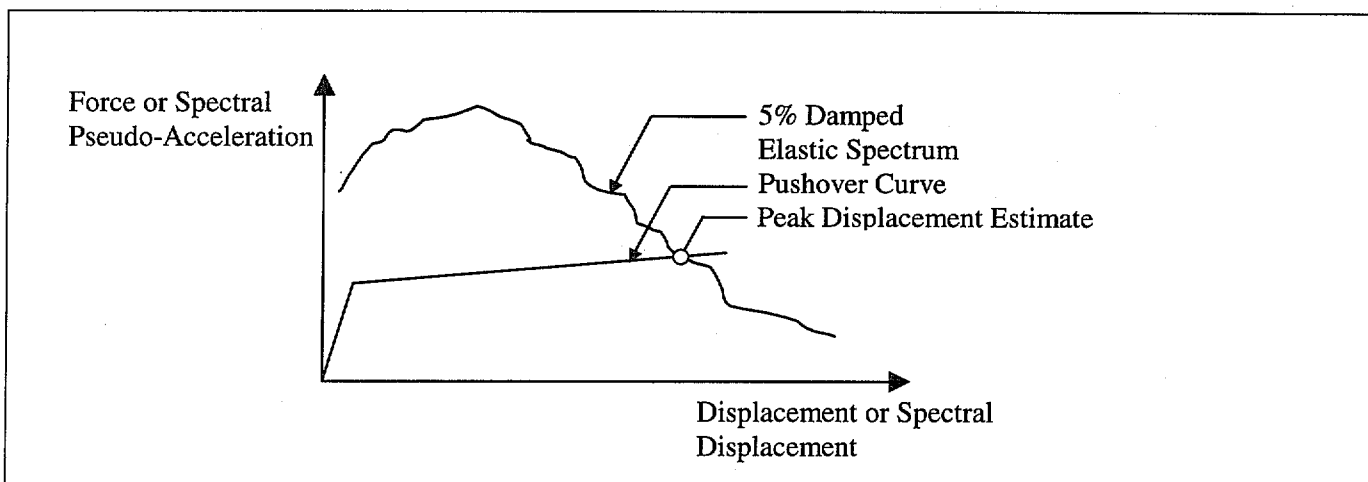


Figure 6-60 Schematic Depiction of Secant Method Displacement Estimation

until the displacements converge. All response-spectrum analyses are made for 5% damping in the secant method, as described in ATC-40. For SDOF structures, the secant method can be implemented in spectral pseudo-acceleration–spectral displacement space, much like the capacity spectrum method. The force/displacement curve may be determined using the constructions of Figure 6-59 for both the undamaged and damaged oscillators. This curve is plotted together with the elastic response spectrum for 5% damping in Figure 6-60. An estimate of peak displacement is indicated in the figure. For the undamaged oscillators, an initial estimate of peak displacement response is the peak response of an elastic oscillator having stiffness equal to the initial stiffness of the oscillator. The intersection of the previous displacement estimate with the idealized force/displacement curve of the structure defines a new secant

stiffness. This stiffness may be used to obtain a revised estimate of peak displacement response. These iterations continue until satisfactory convergence occurs. This is shown schematically in Figure 6-61.

### 6.5.2.3 Capacity Spectrum Method

Like the secant method, the capacity spectrum method assumes that the peak displacement response of a nonlinear system can be estimated by an elastic system having reduced stiffness. The difference is that the elastic spectral-response values are modified to reflect increases in damping associated with inelastic response. A lateral force “pushover” curve is developed for the structure and plotted on spectral pseudo-acceleration–spectral displacement coordinates. The structure is assumed to displace until it reaches an elastic demand curve that has damping that corresponds to a value based on the current displacement estimate.

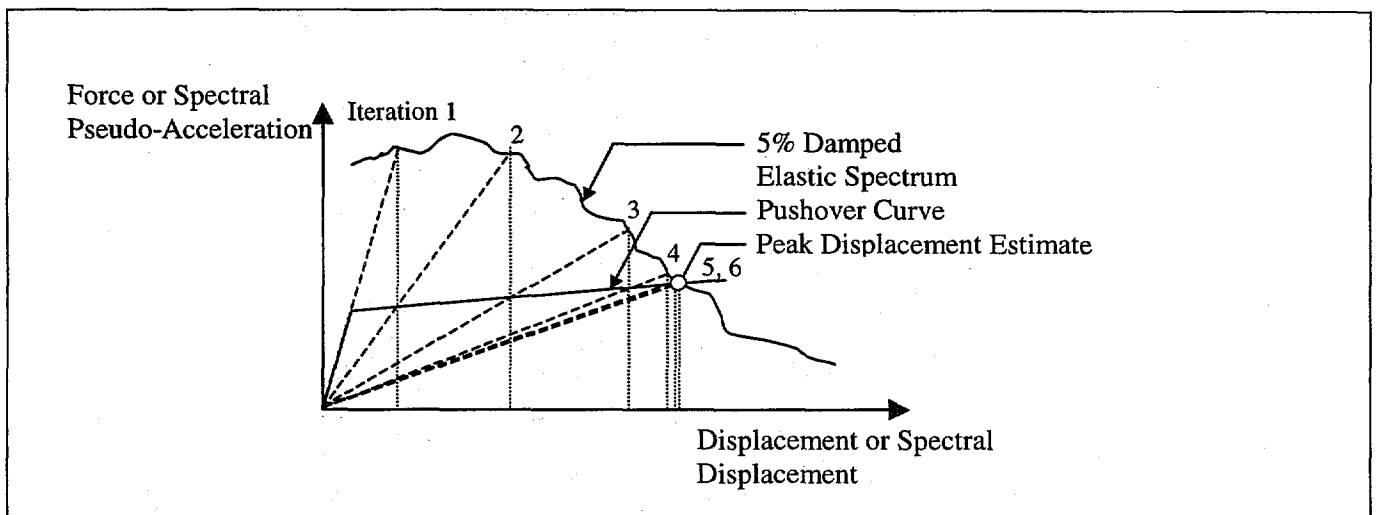


**Figure 6-61** Schematic Depiction of Successive Iterations to Estimate Displacement Response Using the Secant Method for Single-Degree-of-Freedom Oscillators

The method may be implemented by successively iterating displacement response. The initial displacement is estimated using the initial stiffness of the structure and assuming elastic response for damping equal to 5% of critical damping. The intersection of the displacement estimate and the idealized force/displacement curve determines a revised estimate of the secant stiffness. Effective viscous damping is revised prescriptively, based on the displacement estimate. This calculation represents the increase in effective damping with increased hysteretic losses. The iterations continue until satisfactory convergence is obtained. Figure 6-62 illustrates the application of the method.

### 6.5.3 Comments on Procedures

From the above descriptions, it is clear that there are fundamental differences among the various NSPs. The displacement coefficient method primarily relies on the initial effective stiffness to determine a baseline spectral displacement, and it considers strength to a lesser extent for short-period structures.

The secant and capacity spectrum methods are insensitive to initial stiffness (for structures that yield), and displacement estimates depend primarily on yield strength and post-yield stiffness. Effective damping varies with displacement amplitude in the capacity

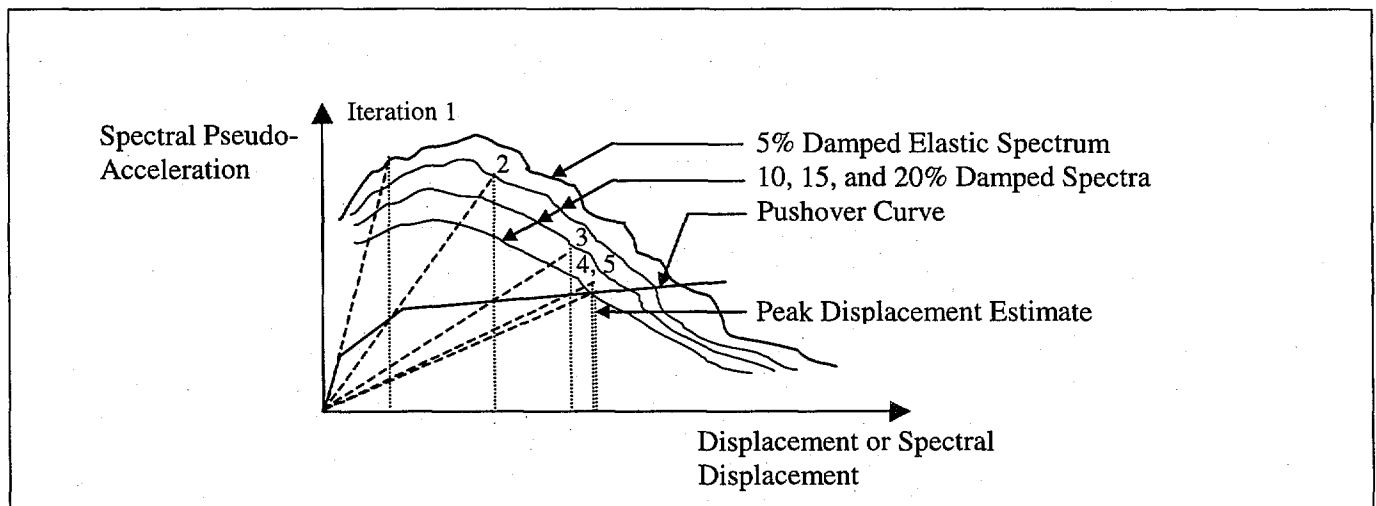


**Figure 6-62** Schematic Depiction of Successive Iterations to Estimate Displacement Response Using the Capacity Spectrum Method

spectrum method, while it is invariant in the secant method. In the form presented in ATC-40, secant method displacement estimates are independent of hysteretic model. Through changes in coefficient  $C_2$ , changes in the force/displacement model may be incorporated in the displacement coefficient method. Differences in hysteresis model are accounted for in the capacity spectrum method adjusting effective damping for three “structural behavior types.”

#### 6.5.4 Application of Procedures to Undamaged and Damaged Oscillators

Each procedure presumes that a smoothed, elastic design response spectrum is to be used in practice. To avoid uncertainties in interpretation of results, the actual pseudo-acceleration spectra were used in place of a smoothed approximation in this study. For the capacity spectrum method, the actual pseudo-acceleration spectra were computed for a range of damping levels, and the spectral reduction factors that are prescribed for use with smoothed design spectra were not employed. These modifications introduce some scatter in the resulting displacement estimates that would not occur if smoothed spectra had been used. Thus, some “smoothing” of the data may be appropriate when interpreting the results.

The NSPs were developed for use with undamaged structures. In this study, the NSPs were applied to the initially-damaged structures using the assumptions described below, representing one of many approaches that can be taken. Recommended procedures for estimating displacements are described in Section 4.4 of FEMA 306.

For the displacement coefficient method, the capacity curve was obtained by the procedure described in FEMA 273. For the uncracked oscillators, a bilinear curve was fit, crossing at 60% of the bilinear curve yield strength. For the damaged oscillators, the effective period of vibration was set at the initial period of the damaged oscillators. Displacements were amplified by the factor  $C_1$  without imposing the optional limit of 2 specified in the provisions.

The secant method was applied iteratively. For undamaged oscillators, the initial stiffness was the yield-point secant stiffness. For damaged oscillators, it was set at the secant stiffness obtained at the displacement imposed by prior ductility demands. The

initial stiffness of the damaged oscillators therefore reflected the previous damage.

The capacity spectrum method was also applied iteratively, beginning with the same initial oscillator stiffness used in the secant method. Effective damping was determined by using the yield point of the undamaged oscillators. The capacity spectrum method was implemented for an intermediate “building characteristic,” identified as Type B. This type is considered to represent average existing buildings subjected to short-duration motions and new buildings subjected to long-duration motions. For this type, effective damping is limited to 29% of critical damping.

For both the capacity spectrum and the secant stiffness methods, 10 iterations were performed for each structure. These iterations generally converged on a single result, and differences in successive approximations were typically less than 1%. On occasion, differences in successive approximations were large, suggesting a lack of convergence due to the jagged nature of the actual (not smoothed) spectra. Where these differences occurred, the displacement estimate at the tenth iteration was retained.

## 6.6 Comparison of NSP and Dynamic Analysis Results

### 6.6.1 Introduction

In evaluating the utility of the NSPs, attention may be directed at two estimates. The first is peak displacement response; it could be expected that an acceptable procedure would estimate the peak displacement response,  $d_d$ , of a nonlinear system within acceptable limits of accuracy. Second, it is possible that a procedure may be systematically biased, and hence may estimate displacement response poorly while providing reasonable estimates of displacement ratio; that is, the ratio of damaged structure displacement to undamaged structure displacement,  $d'_d/d_d$ . These response indices,  $d_d$  and  $d'_d/d_d$ , are examined in detail in the following sections for Takeda oscillators designed for bilinear DDDs of 8.

### 6.6.2 Displacement Estimation

Peak displacement response of the undamaged Takeda oscillators was estimated for each earthquake record. The ratio of the peak displacement estimate from NSP

and the value computed for each Takeda5 oscillator, at each period and for each ground motion record, is plotted in Figure 6-63 for  $DDD = 8$  and  $RSR = 1$ . The log scale plots the ratio of estimated and computed displacement,  $d_{d,NSP}/d_d$ . Plots are presented for each ground motion category and for each NSP.

In Figure 6-63, it can be observed that the ratio of the estimated and computed displacements,  $d_{d,NSP}/d_d$ , can vary significantly, ranging from less than 0.3 to more than 100. At any period ratio, the ratio  $d_{d,NSP}/d_d$  may approach or exceed an order of magnitude. Because the trends tend to be consistent for each ground motion record, the jaggedness of the actual spectra does not appear to be the source of most of the variability.

Figure 6-64 plots mean values of ratios  $d_{d,NSP}/d_d$  determined for each NSP, for all ground motions and all  $DDD$  values. Results for short- and long-period Takeda5 oscillators are plotted separately. In Figure 6-64, it can be observed that the NSP procedures tend to overestimate, in a mean sense, the displacements computed for the short-period Takeda5 oscillators for all  $DDD$ . Takeda oscillators having  $DDD = 1$  often displaced less than their bilinear counterparts because the Takeda oscillators had initial stiffness equal to twice that of their bilinear counterparts. The difference in initial stiffness explains the tendency of the NSP methods to overestimate displacements for low  $DDD$ . This is particularly true for the secant method estimates of short-period oscillators, for which mean ratios exceeded six for  $DDD$  greater than 1. The period ratio,  $T_e/T_g$ , marking the boundary of the elevated estimates tends to be less than one, possibly reflecting the effective increase in period of Takeda5 oscillators as their stiffness reduces (Figure 6-63).

Figure 6-64 indicates that each NSP tends to overestimate the displacement response of short-period oscillators and that the capacity spectrum method is most accurate for long-period Takeda5 oscillators, in a mean sense. Nevertheless, Figure 6-63 indicates the substantial variability in displacement estimates and the potential to overestimate or underestimate displacements with all methods. A single estimate cannot capture the breadth of response variability that may occur at a given site.

Based on Figures 6-63 and 6-64, the coefficient and capacity spectrum methods appear to be reasonably accurate and to have the least scatter. The secant method

tended to overestimate displacement and exhibited more scatter in values of  $d_{d,NSP}/d_d$ .

### 6.6.3 Displacement Ratio Estimation

The ratio of damaged oscillator displacement,  $d'_d$ , and the displacement of the corresponding Takeda oscillator having no initial damage,  $d_d$ , was estimated using the NSP methods for each Takeda oscillator/earthquake pair, as described in Section 6.5.4. This estimated displacement ratio is compared with the ratio computed from the dynamic analyses in Figures 6-65 through 6-73.

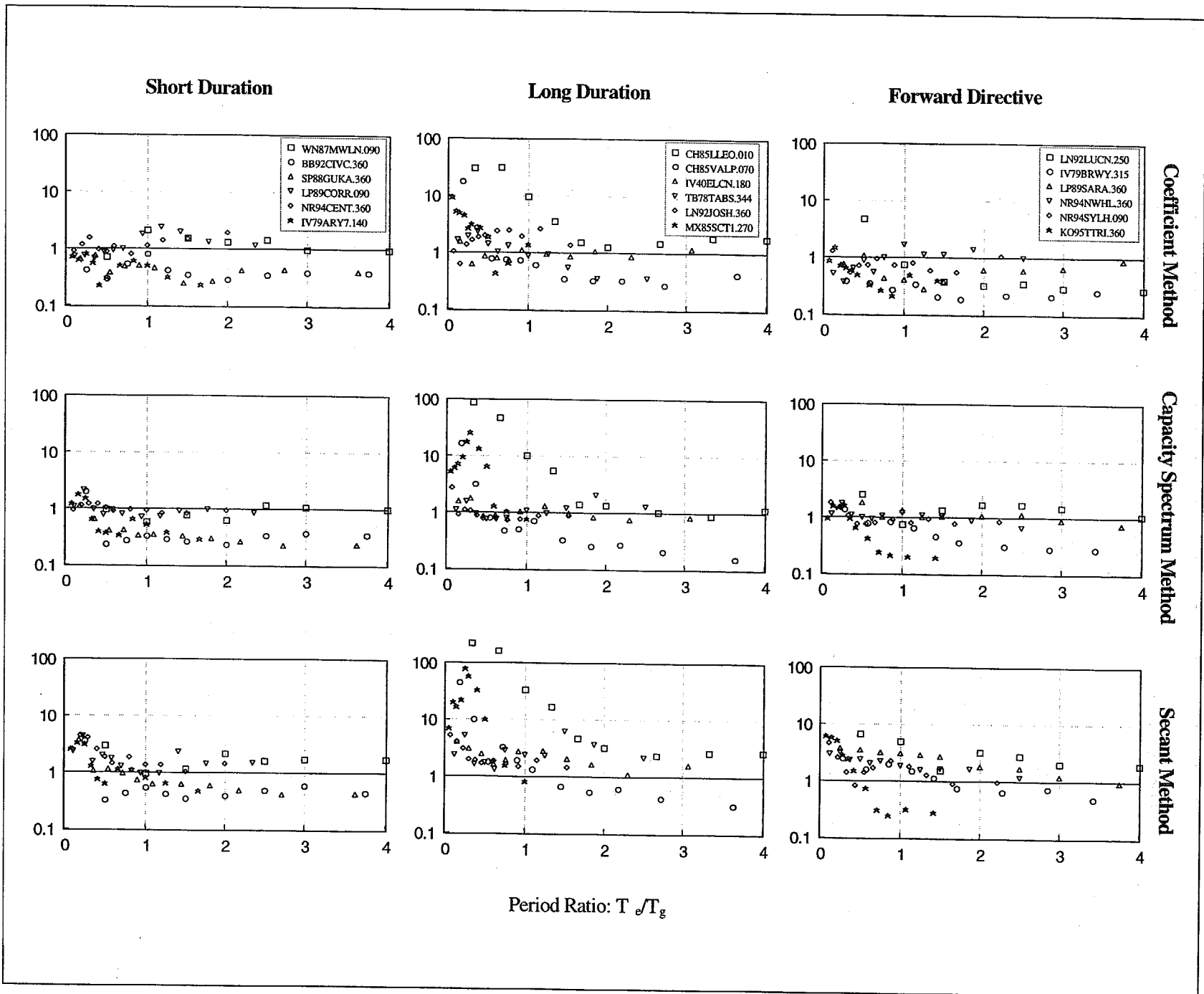
It can be observed that simple application of the displacement coefficient method using the initial stiffness of the undamaged oscillator to calculate  $d_d$  and using the reduced stiffness of the damaged oscillator to calculate  $d'_d$  almost always overestimates the effects of damage for the cases considered.

Application of the secant and capacity spectrum methods, using the initial and reduced stiffness values, typically led to nearly identical displacement estimates: estimates of  $d'_d/d_d$  were often approximately equal to one. Figures 6-68 through 6-73, which might appear to testify to the success of the methods, instead tend more to represent the inverse of the  $d'_d/d_d$  as computed for the Takeda models. Figures 6-38 through 6-40 indicate that computed values of  $d_d/d'_d$  should tend to be around one, decreasing slightly for small periods.

The preceding plots examine the effectiveness of the methods, as implemented here, for estimating the consequences of prior ductility demand. It is also of interest to examine the effectiveness of the methods in accounting for strength loss. To do this, the ratio of the displacement obtained with  $RSR = 0.6$  to that with  $RSR = 1.0$  was evaluated for the nonlinear Takeda5 oscillators having  $DDD = 8$  and  $PDD = 1$ , in order to compare the NSP estimates of the displacement ratio with the displacement ratio computed for the nonlinear Takeda5 oscillators. The upper plots in Figures 6-74 through 6-82 show the estimated displacement ratio for one of the three NSPs, and the lower plots of these figures normalize this displacement ratio by the displacement ratio computed for the Takeda5 oscillators. It can be observed that the NSP methods tend to account correctly for the effect of strength reduction on displacement response, in a mean sense.

(Text continued on page 177)





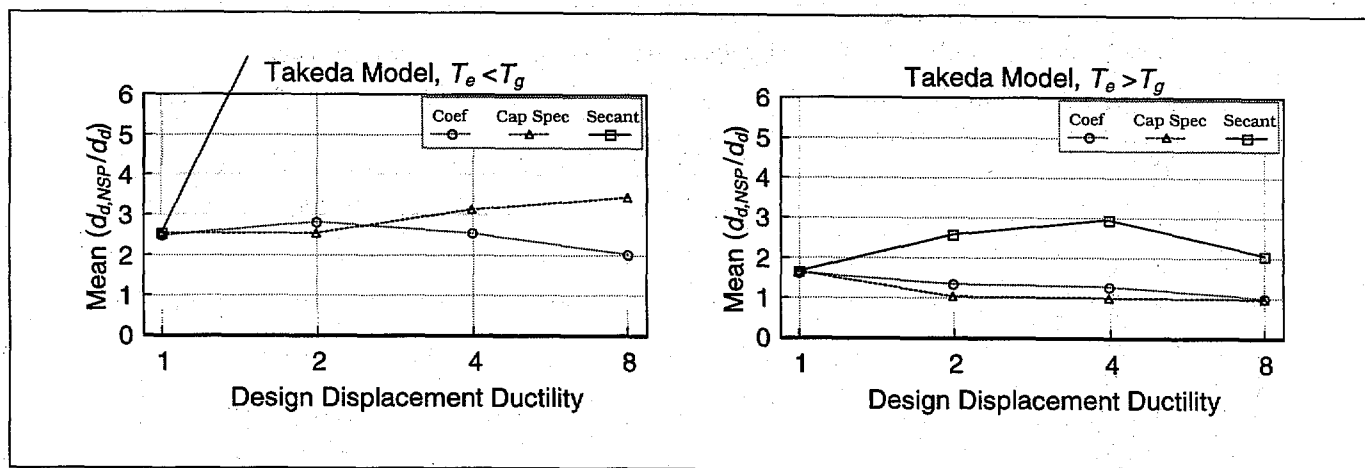


Figure 6-64 Mean values of  $d_{d,NSP}/d_d$  for all ground motions for each NSP method, for short and long-period Takeda5 Models. See text in Section 6.6.2.

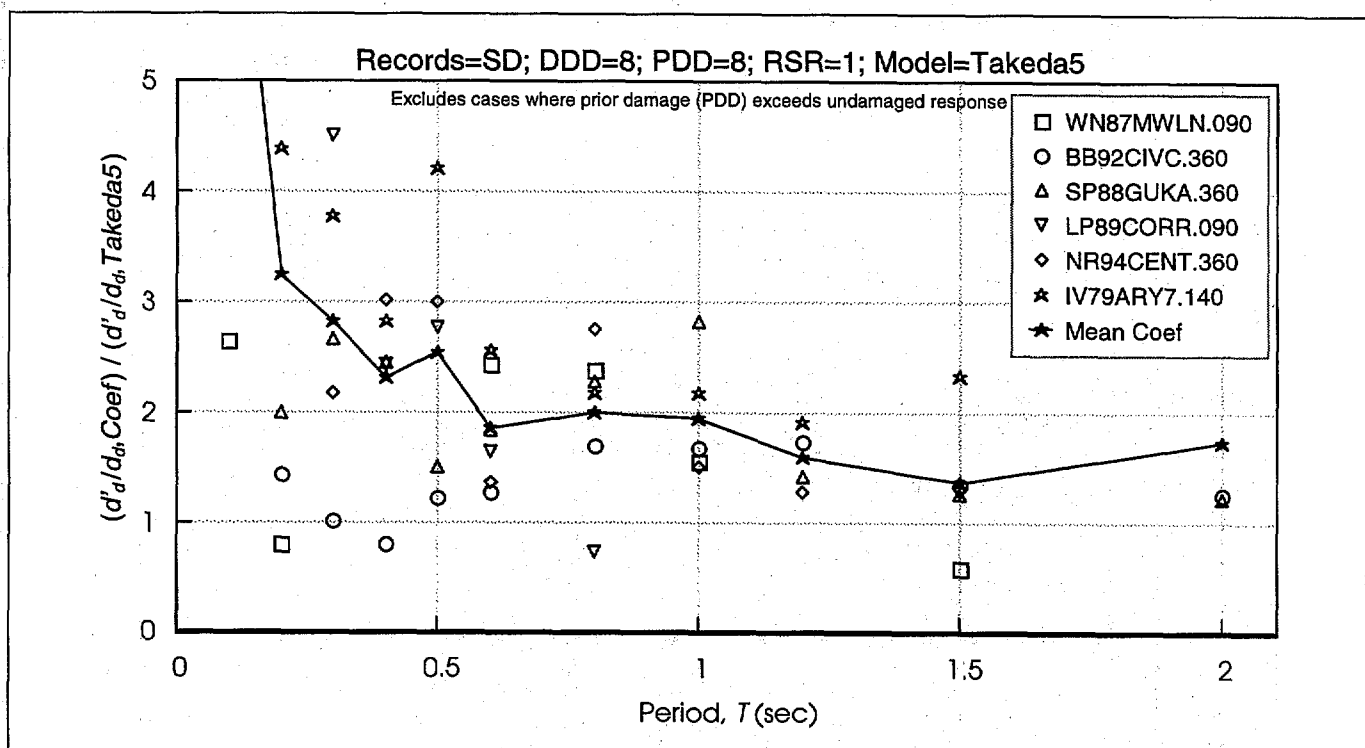
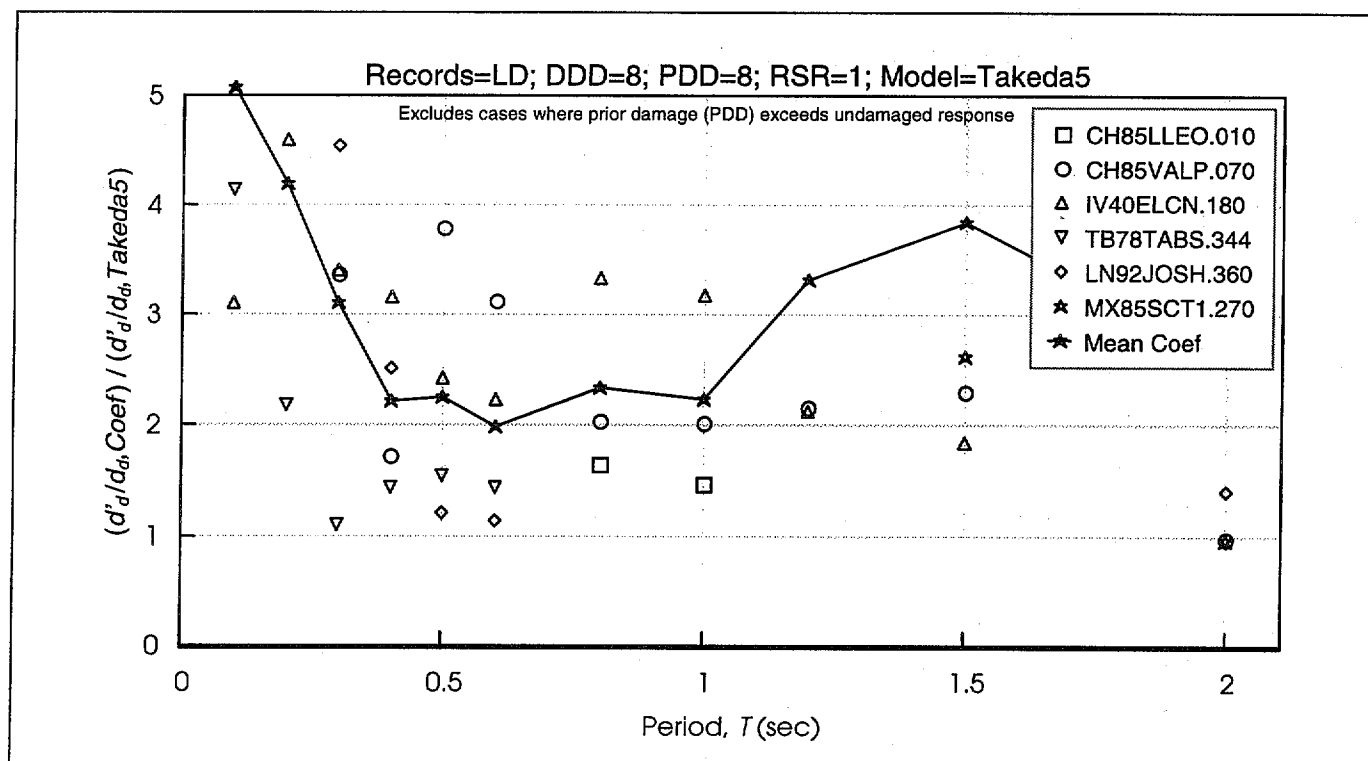
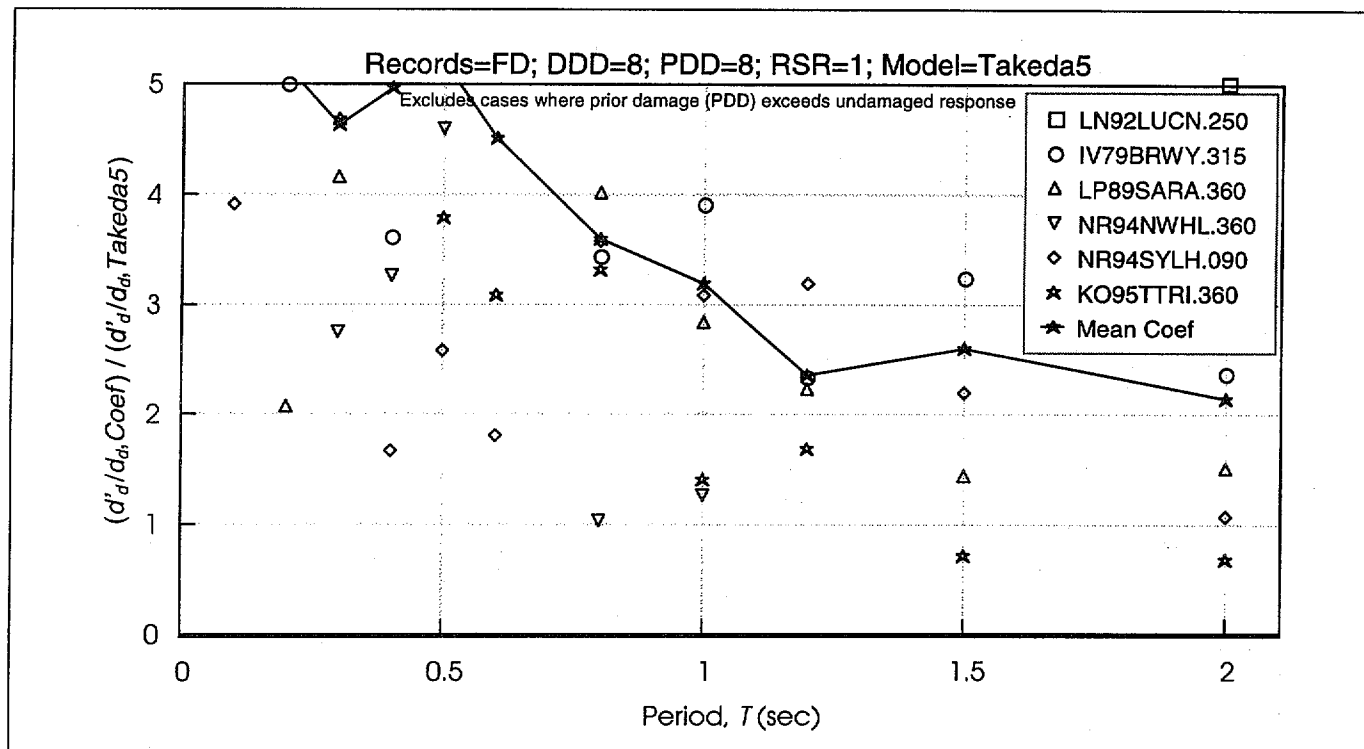


Figure 6-65 Coefficient Method Estimates of Ratio of Damaged and Undamaged Oscillator Displacement Normalized by Computed Ratio, for Short-Duration Records  
 DDD = Design Displacement Ductility; PDD = Prior Ductility Demand; RSR = Reduced Strength Ratio



**Figure 6-66** Coefficient Method Estimates of Ratio of Damaged and Undamaged Oscillator Displacement Normalized by Computed Ratio, for Long-Duration Records  
 DDD = Design Displacement Ductility; PDD = Prior Ductility Demand; RSR = Reduced Strength Ratio



**Figure 6-67** Coefficient Method Estimates of Ratio of Damaged and Undamaged Oscillator Displacement Normalized by Computed Ratio, for Forward Directive Records  
 DDD = Design Displacement Ductility; PDD = Prior Ductility Demand; RSR = Reduced Strength Ratio

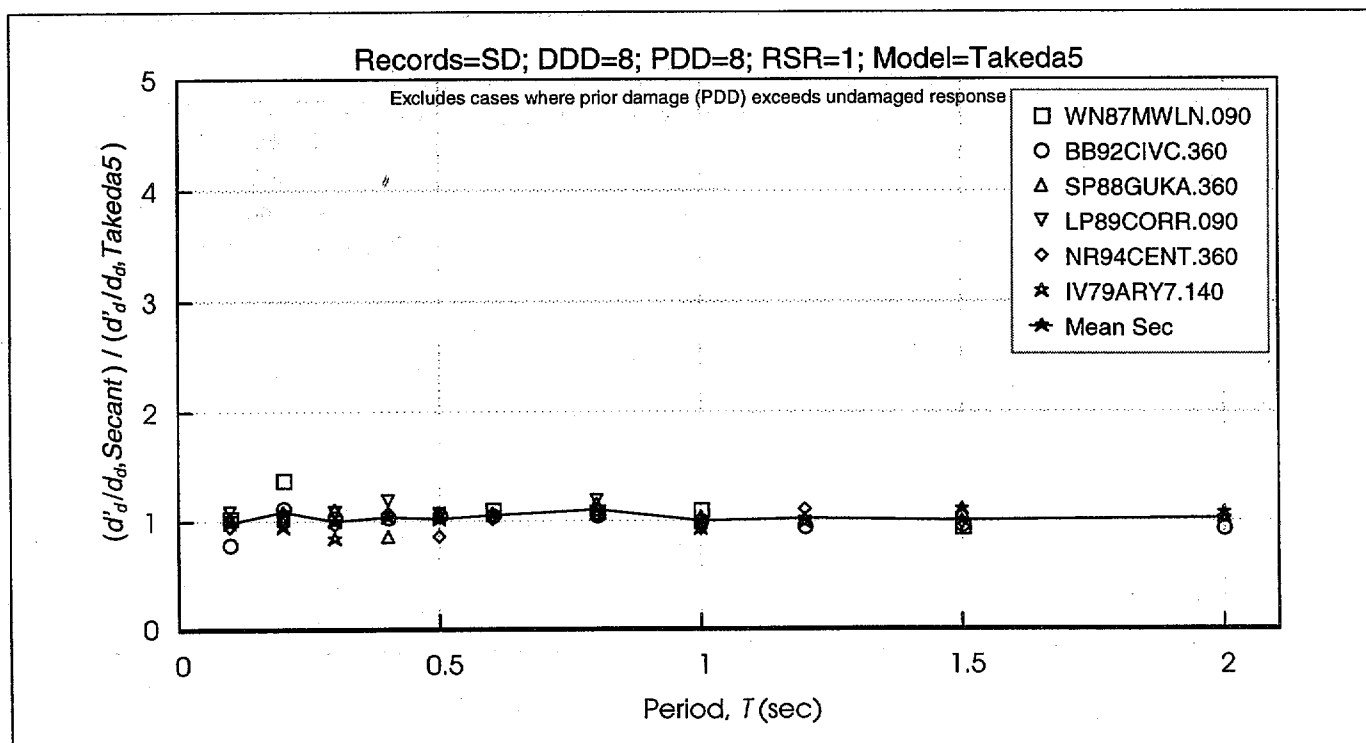


**Figure 6-68** Secant Method Estimates of Ratio of Damaged and Undamaged Oscillator Displacement Normalized by Computed Ratio, for Short-Duration Records  
 DDD = Design Displacement Ductility; PDD = Prior Ductility Demand; RSR = Reduced Strength Ratio

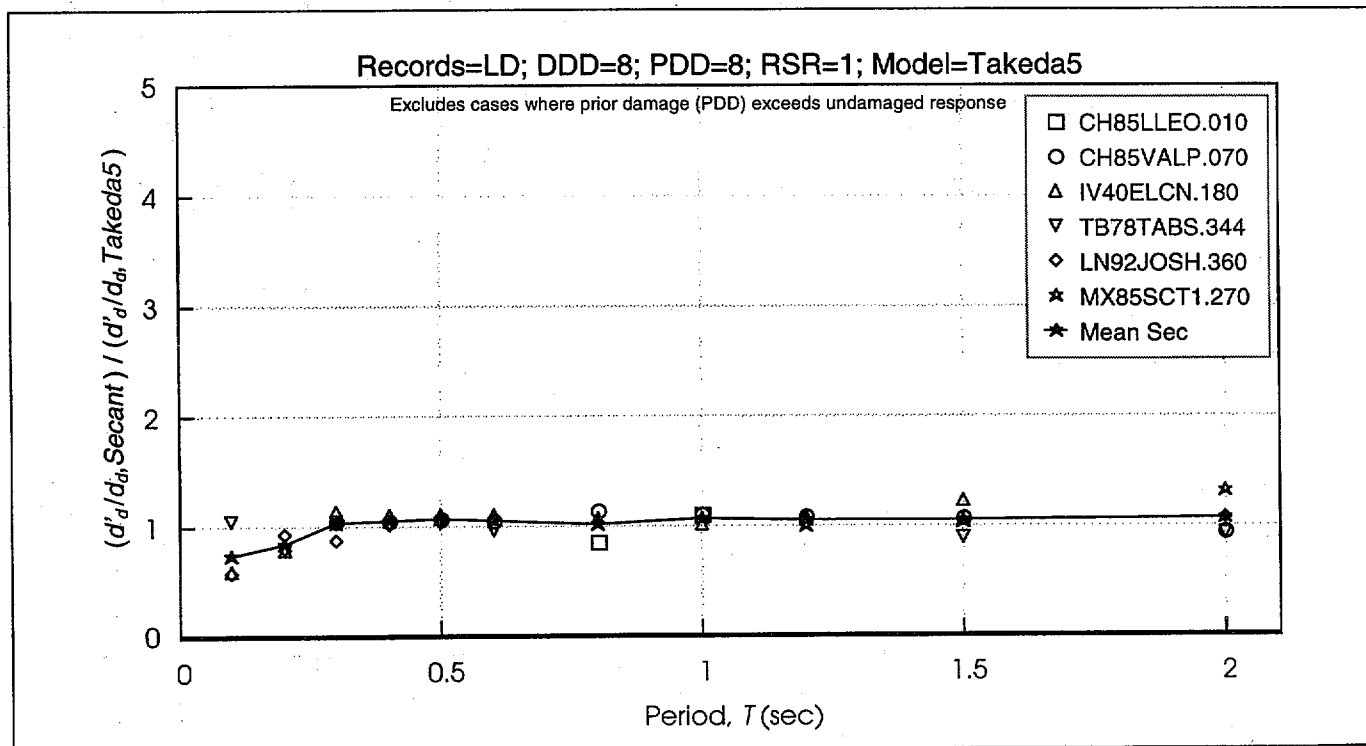


**Figure 6-69** Secant Method Estimates of Ratio of Damaged and Undamaged Oscillator Displacement Normalized by Computed Ratio, for Long-Duration Records  
 DDD = Design Displacement Ductility; PDD = Prior Ductility Demand; RSR = Reduced Strength Ratio

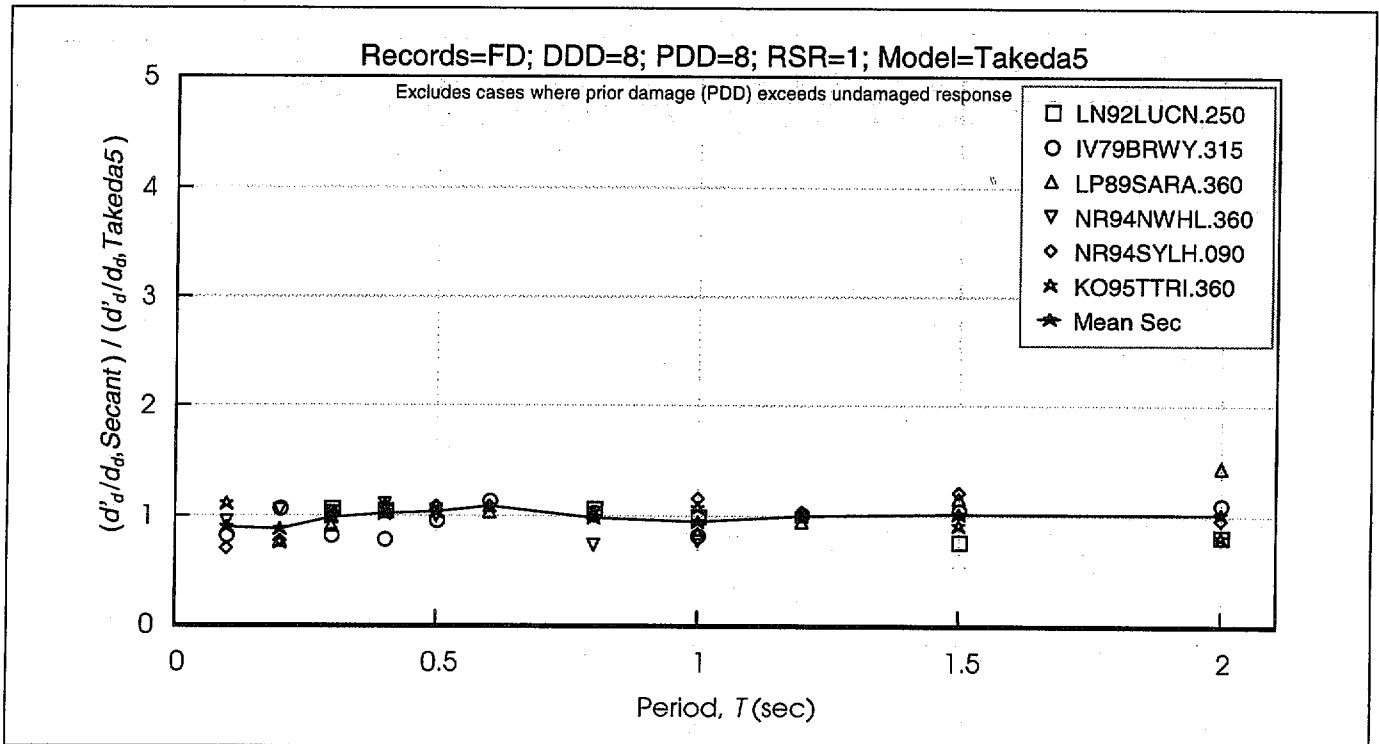


**Figure 6-70** Secant Method Estimates of Ratio of Damaged and Undamaged Oscillator Displacement Normalized by Computed Ratio, for Forward Directive Records  
 DDD = Design Displacement Ductility; PDD = Prior Ductility Demand; RSR = Reduced Strength Ratio

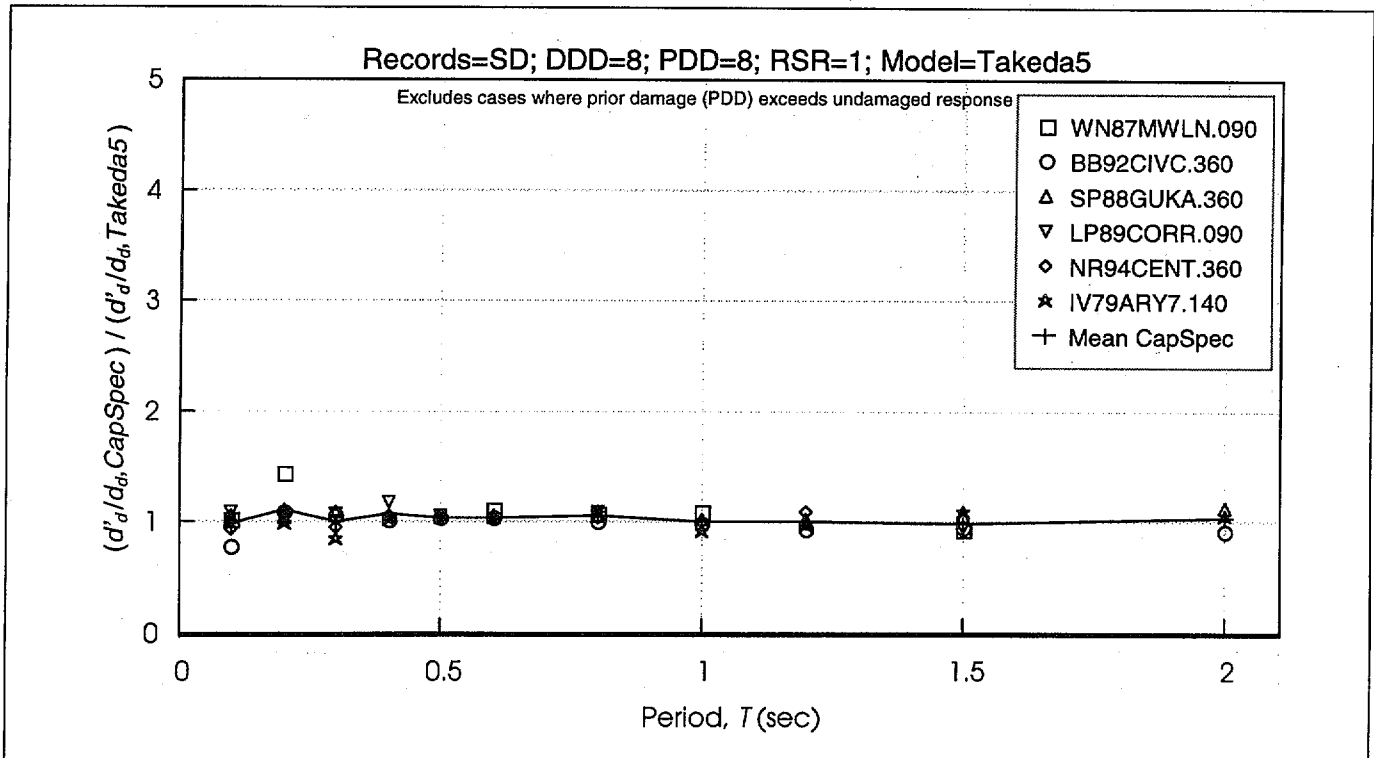


**Figure 6-71** Capacity Spectrum Method Estimates of Ratio of Damaged and Undamaged Oscillator Displacement Normalized by Computed Ratio, for Short-Duration Records  
 DDD = Design Displacement Ductility; PDD = Prior Ductility Demand; RSR = Reduced Strength Ratio

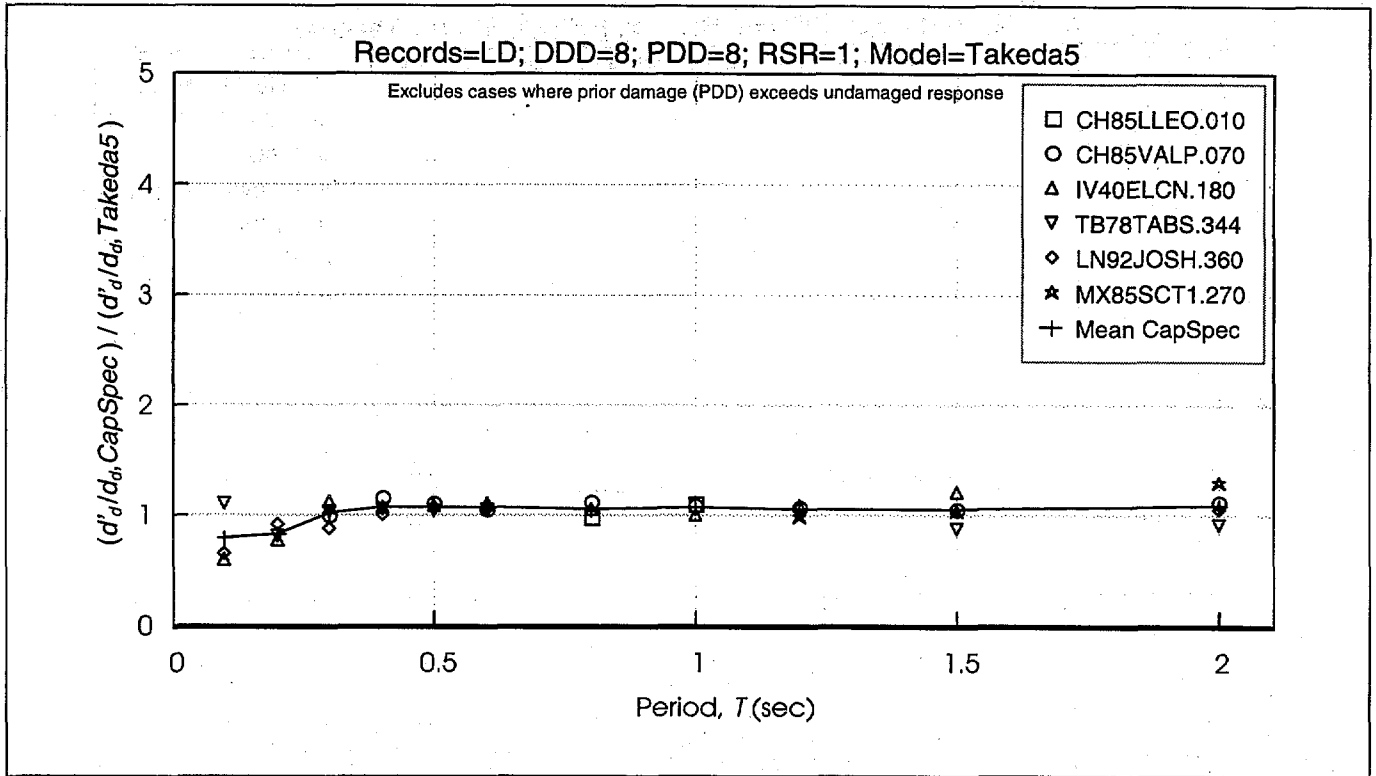


**Figure 6-72** Capacity Spectrum Method Estimates of Ratio of Damaged and Undamaged Oscillator Displacement Normalized by Computed Ratio, for Long-Duration Records  
 DDD = Design Displacement Ductility; PDD = Prior Ductility Demand; RSR = Reduced Strength Ratio

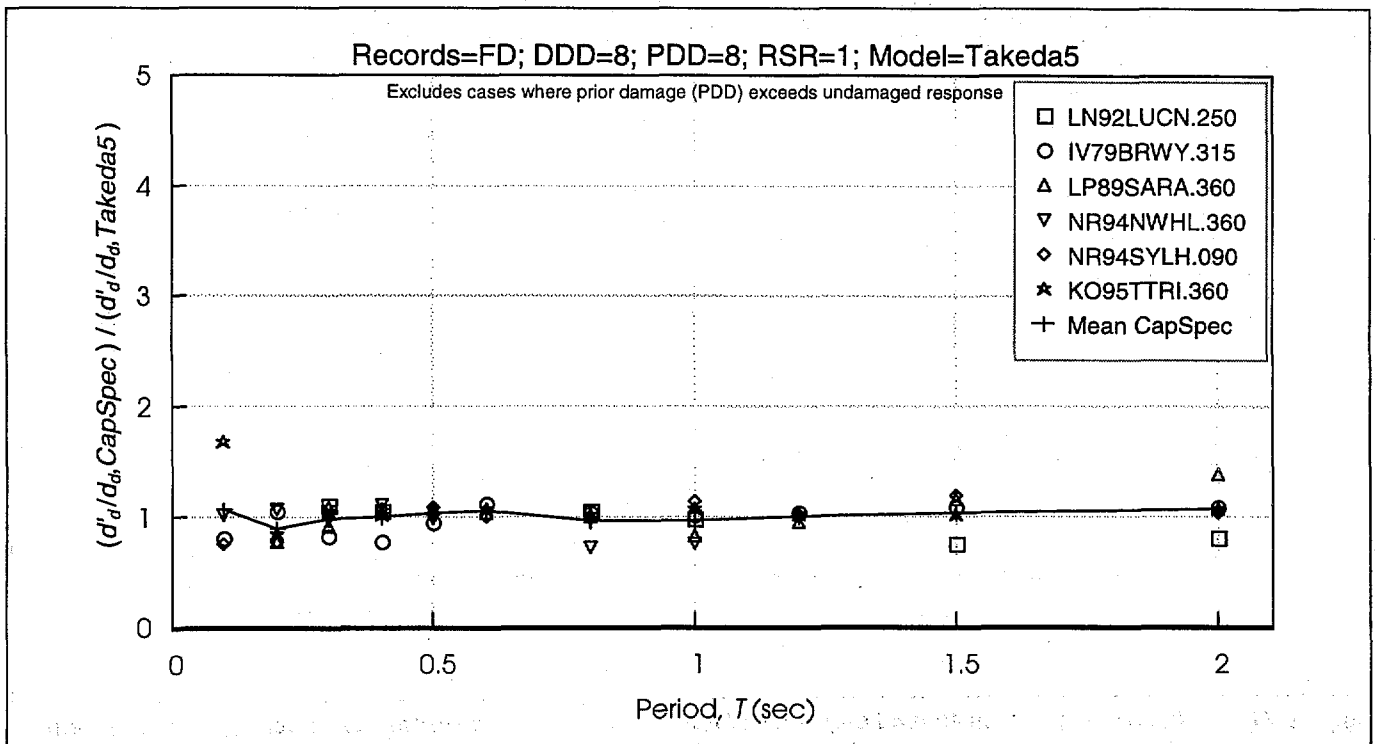


**Figure 6-73** Capacity Spectrum Method Estimates of Ratio of Damaged and Undamaged Oscillator Displacement Normalized by Computed Ratio, for Forward Directive Records  
 DDD = Design Displacement Ductility; PDD = Prior Ductility Demand; RSR = Reduced Strength Ratio

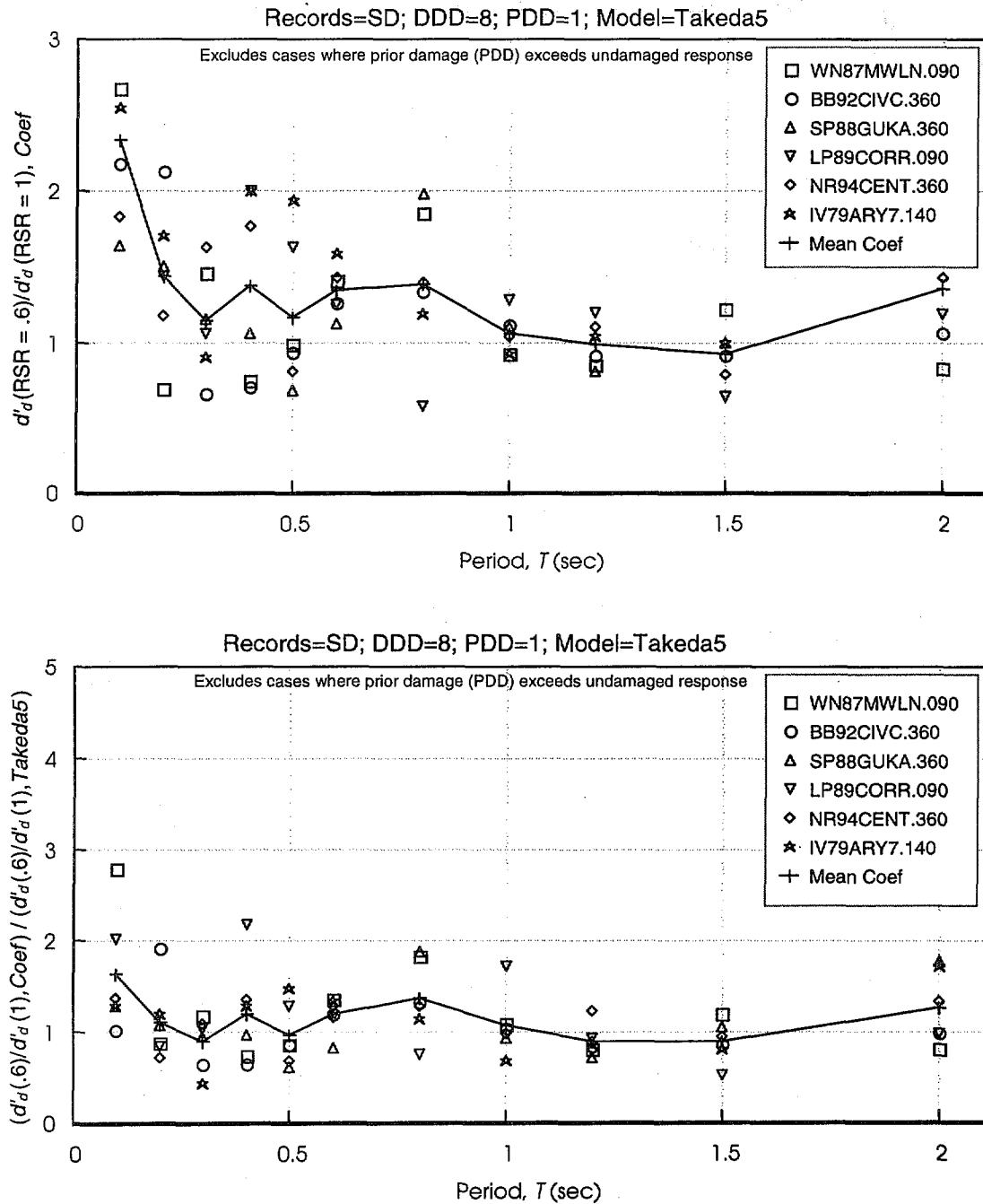


Figure 6-74

**Coefficient Method Estimates of Displacement Ratio of RSR=0.6 and RSR=1.0 Takeda5 Oscillators having DDD= 8 and PDD= 1**

DDD = Design Displacement Ductility; PDD = Prior Ductility Demand; RSR = Reduced Strength Ratio

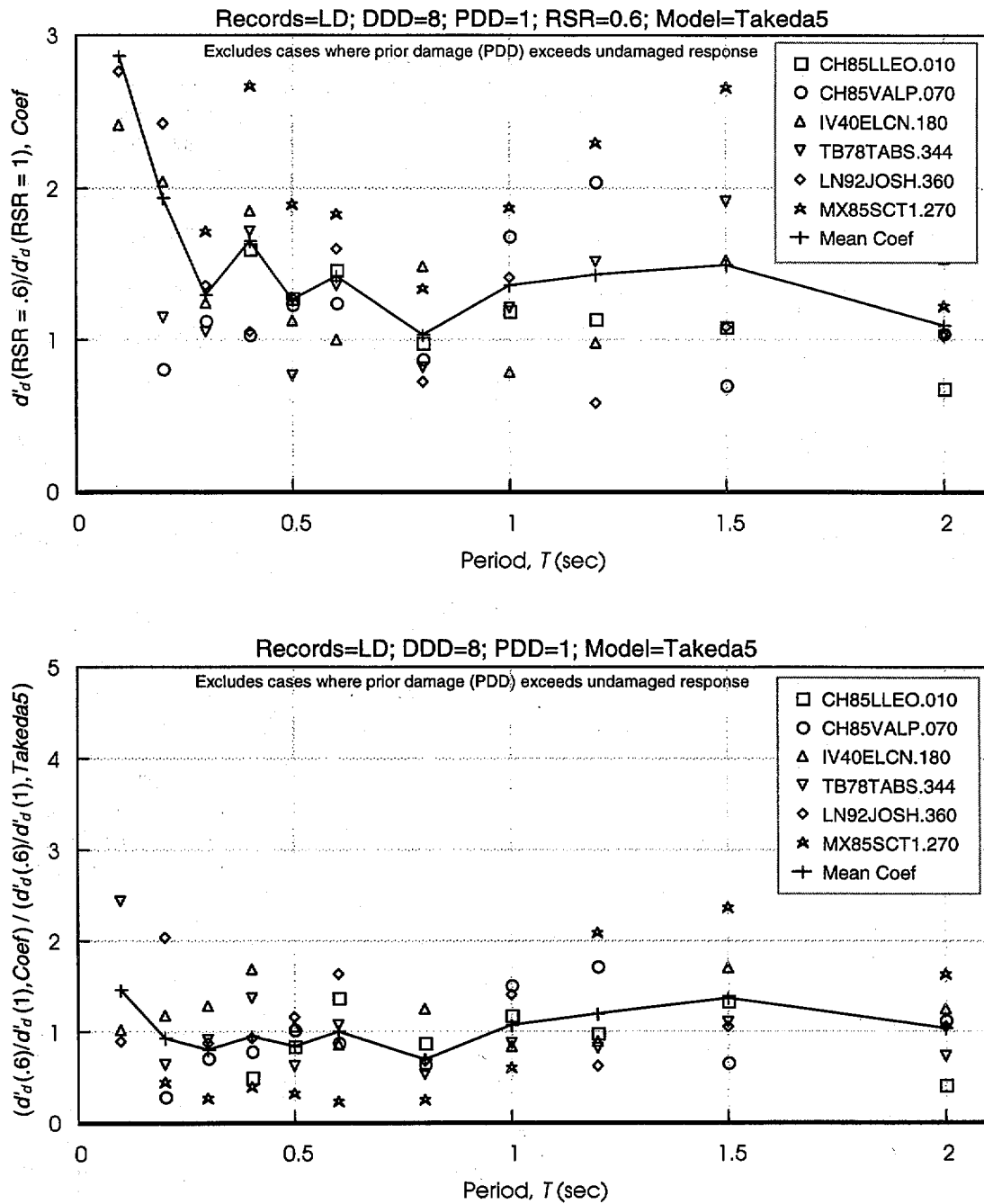
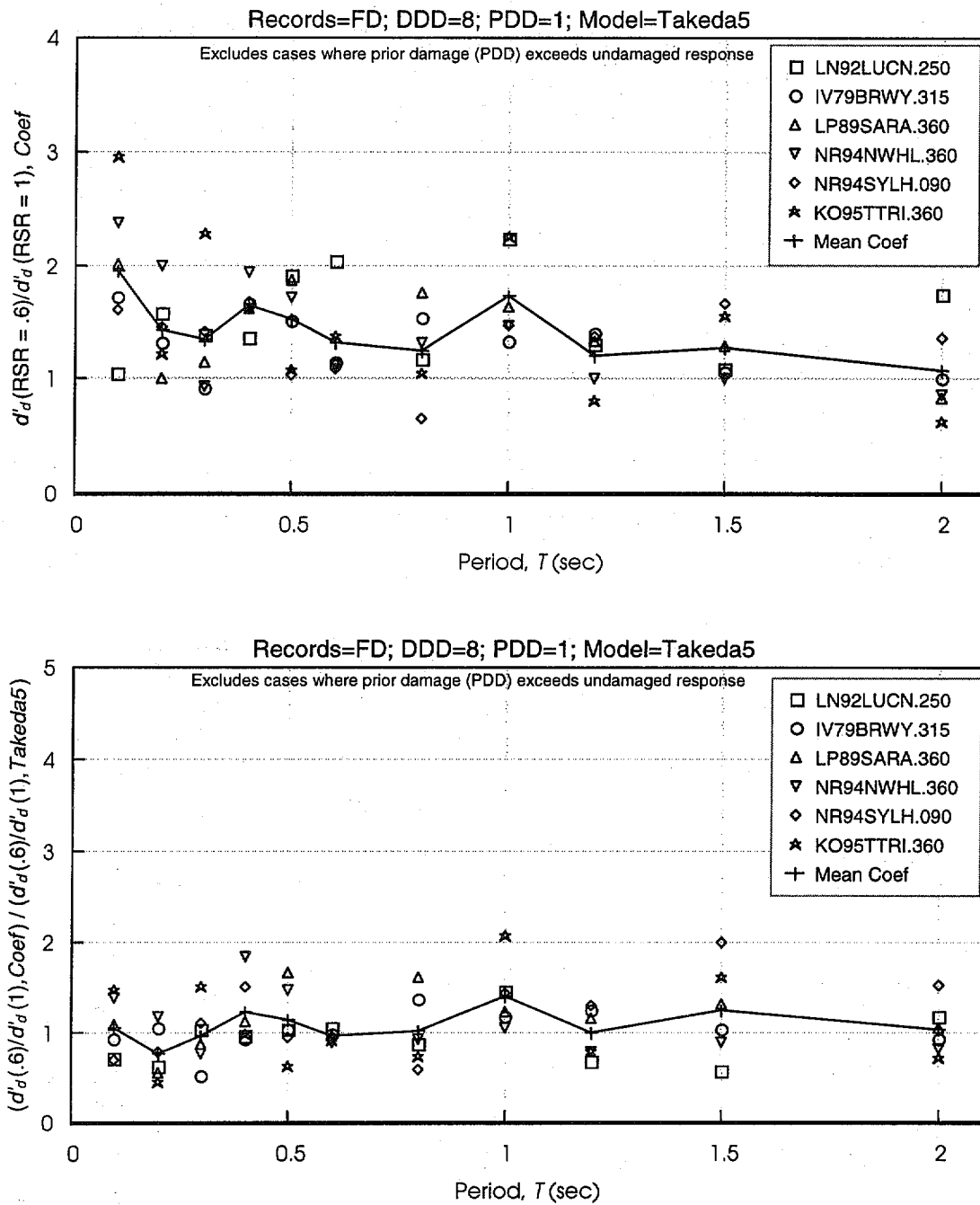


Figure 6-75

**Coefficient Method Estimates of Displacement Ratio of RSR=0.6 and RSR=1.0 Takeda5 Oscillators having DDD= 8 and PDD= 1**  
 DDD = Design Displacement Ductility; PDD = Prior Ductility Demand; RSR = Reduced Strength Ratio





**Figure 6-76** Coefficient Method Estimates of Displacement Ratio of RSR=0.6 and RSR=1.0 Takeda5 Oscillators having DDD= 8 and PDD= 1  
 DDD = Design Displacement Ductility; PDD = Prior Ductility Demand; RSR = Reduced Strength Ratio

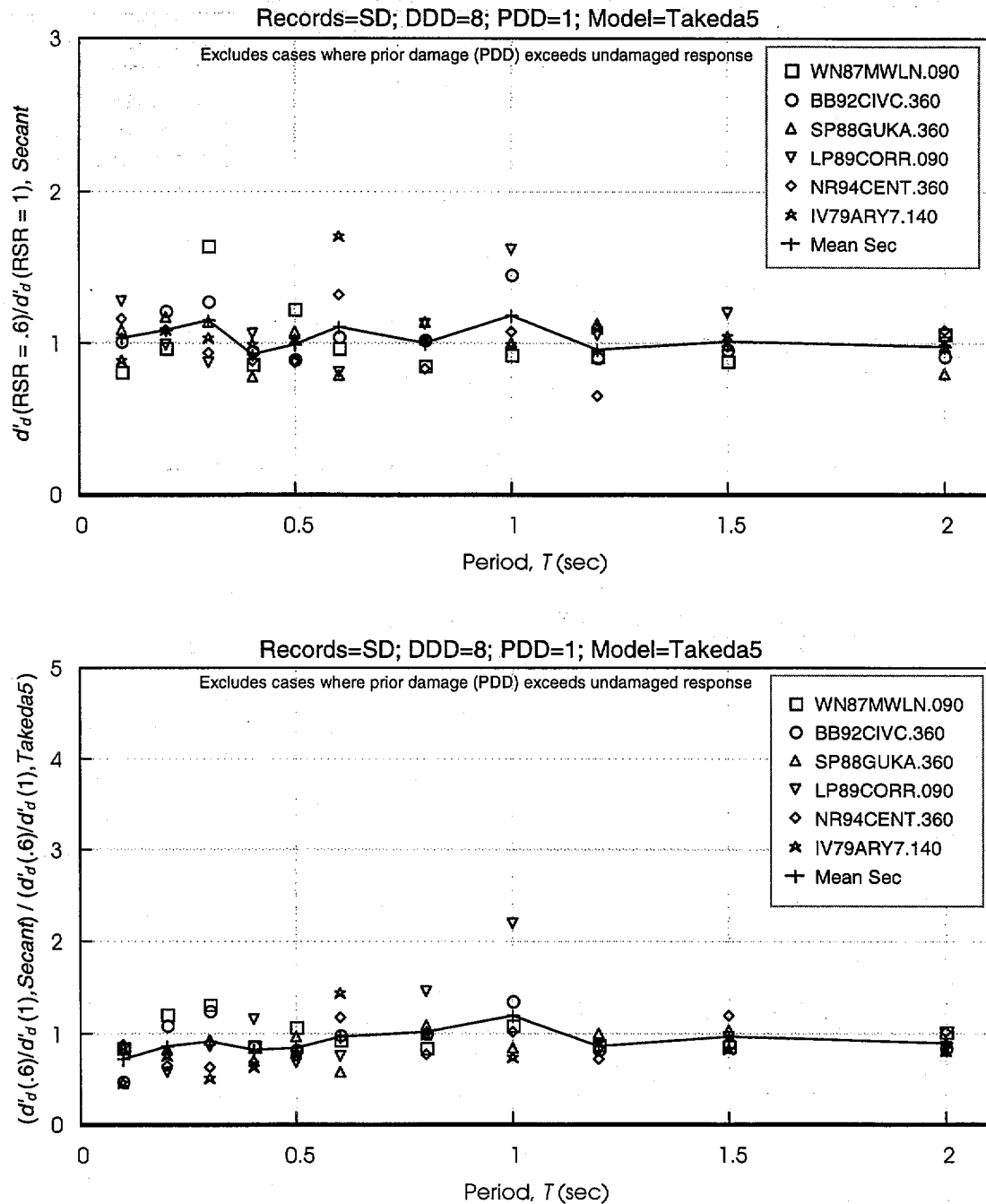


Figure 6-77 Secant Method Estimates of Displacement Ratio of RSR=0.6 and RSR=1.0 Takeda5 Oscillators having DDD= 8 and PDD= 1  
 DDD = Design Displacement Ductility; PDD = Prior Ductility Demand; RSR = Reduced Strength Ratio

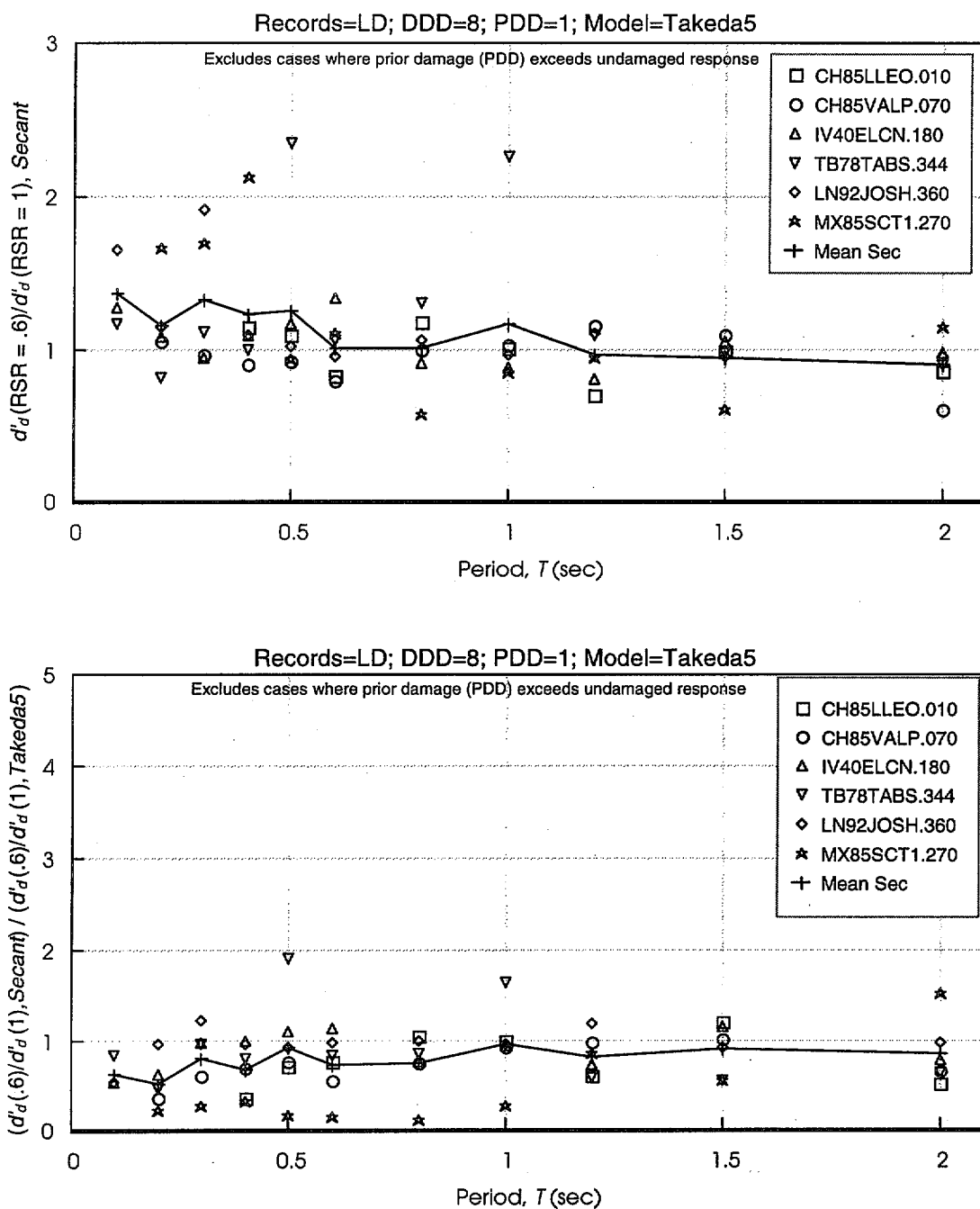
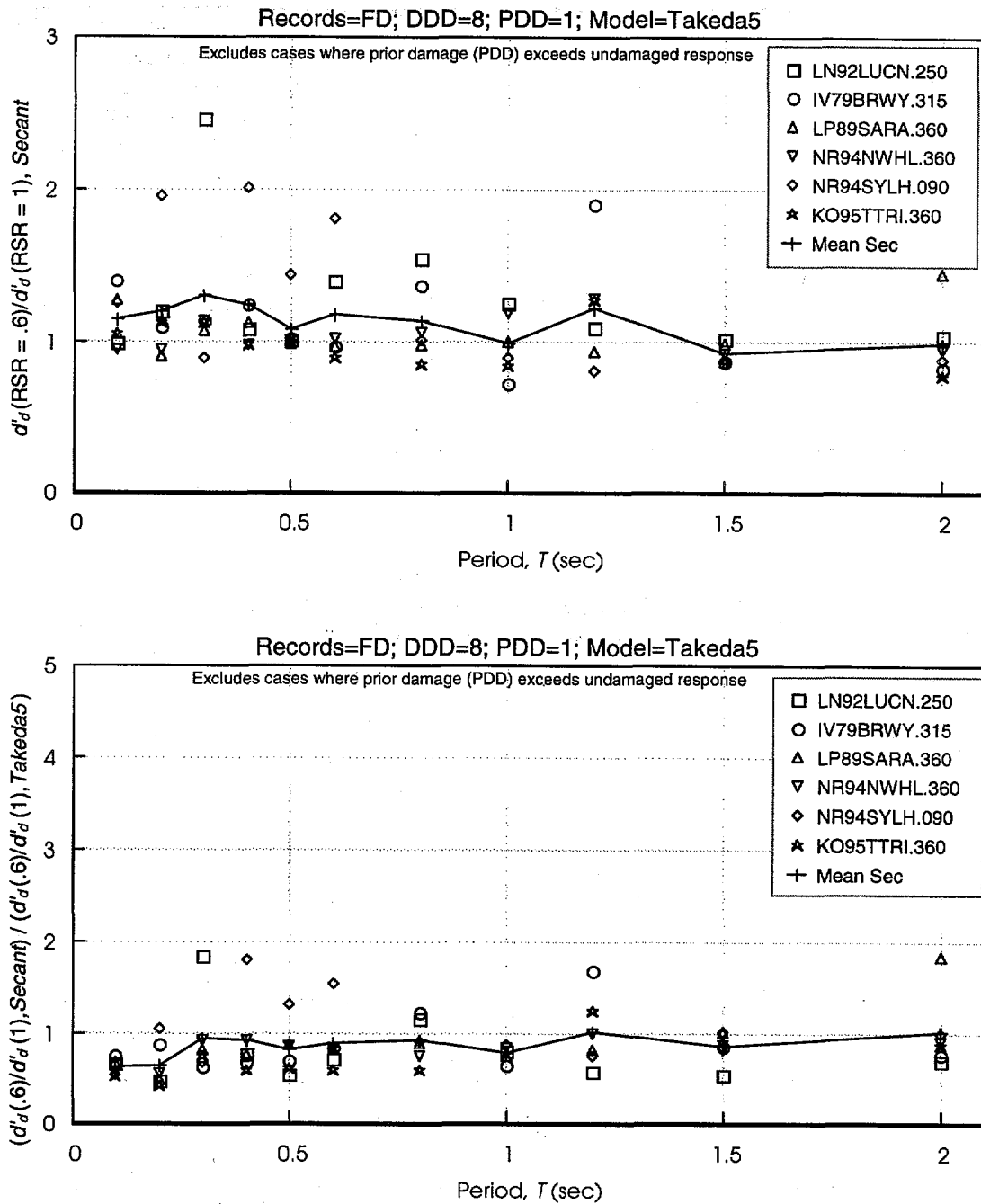


Figure 6-78 Secant Method Estimates of Displacement Ratio of RSR=0.6 and RSR=1.0 Takeda5 Oscillators having DDD= 8 and PDD= 1  
 DDD = Design Displacement Ductility; PDD = Prior Ductility Demand; RSR = Reduced Strength Ratio



**Figure 6-79** Secant Method Estimates of Displacement Ratio of RSR=0.6 and RSR=1.0 Takeda5 Oscillators having DDD= 8 and PDD= 1  
 DDD = Design Displacement Ductility; PDD = Prior Ductility Demand; RSR = Reduced Strength Ratio

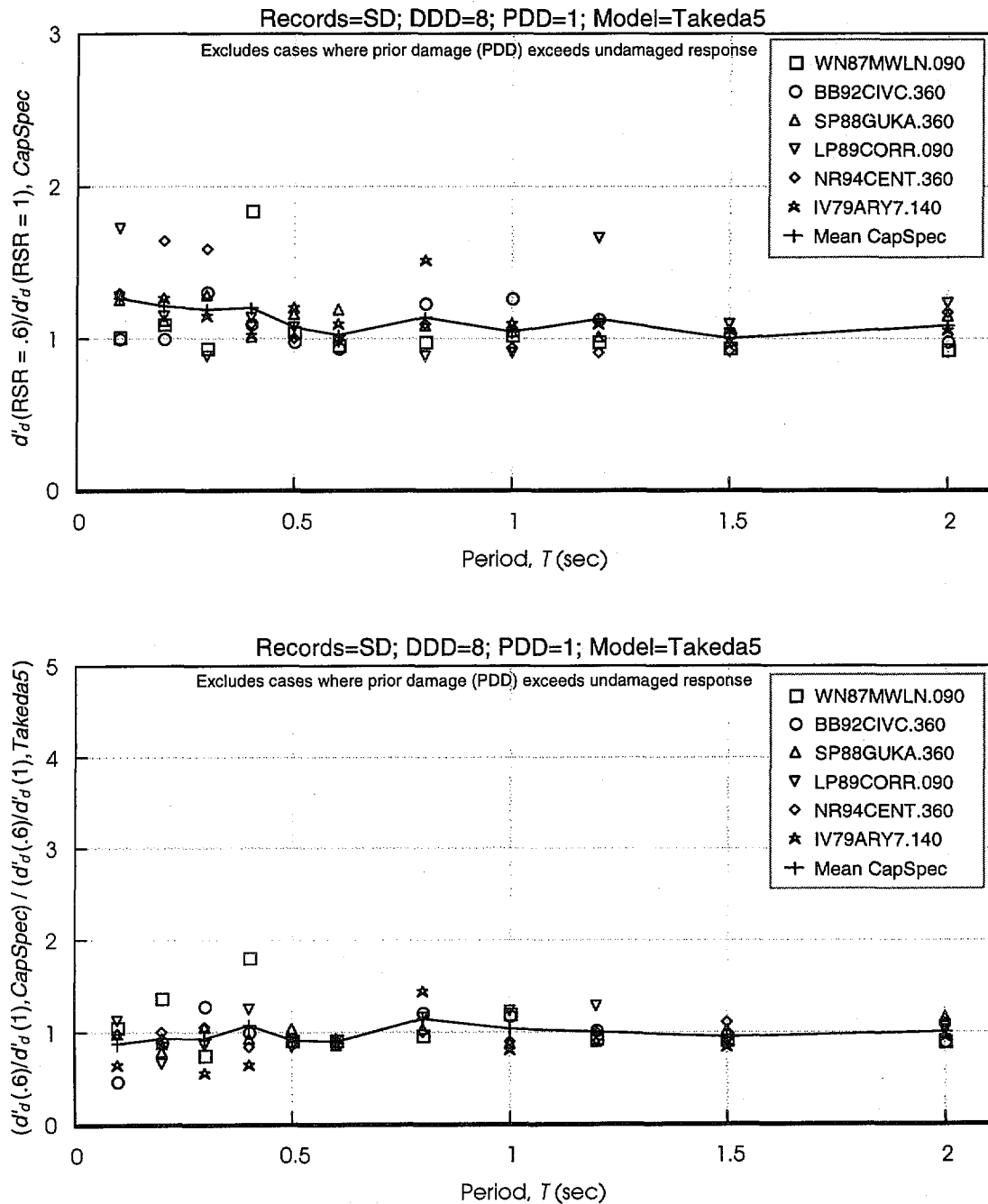
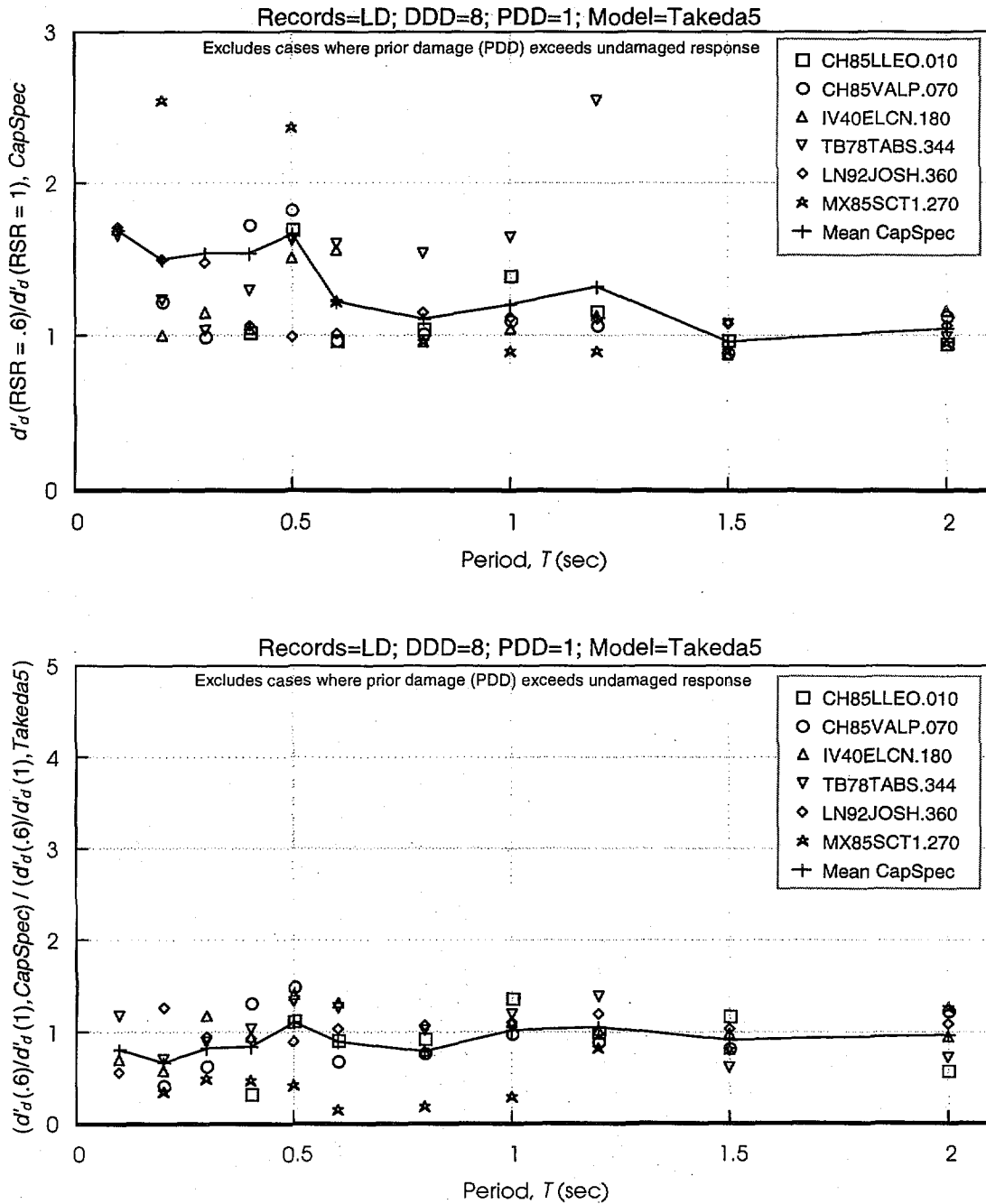
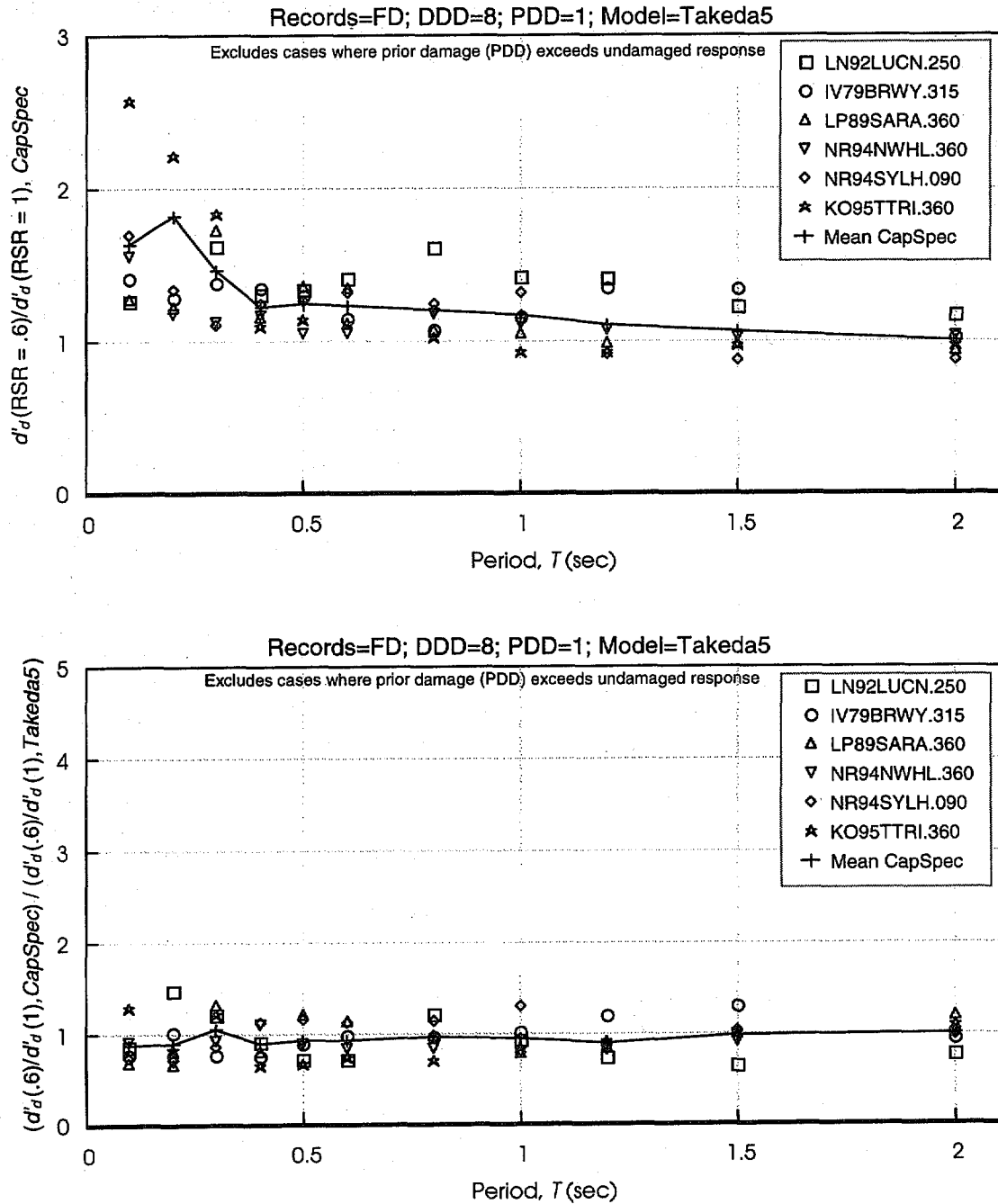


Figure 6-80 Capacity Spectrum Method Estimates of Displacement Ratio of  $RSR=0.6$  and  $RSR=1.0$  Takeda5 Oscillators having  $DDD=8$  and  $PDD=1$   
 $DDD$  = Design Displacement Ductility;  $PDD$  = Prior Ductility Demand;  $RSR$  = Reduced Strength Ratio



**Figure 6-81** Capacity Spectrum Method Estimates of Displacement Ratio of RSR=0.6 and RSR=1.0 Takeda5 Oscillators having DDD= 8 and PDD= 1  
DDD = Design Displacement Ductility; PDD = Prior Ductility Demand; RSR = Reduced Strength Ratio



**Figure 6-82** Capacity Spectrum Method Estimates of Displacement Ratio of RSR=0.6 and RSR=1.0 Takeda5 Oscillators having DDD= 8 and PDD= 1  
 DDD = Design Displacement Ductility; PDD = Prior Ductility Demand; RSR = Reduced Strength Ratio

## 6.7 Conclusions and Implications

The analyses presented indicate that the displacement response characteristics of the ground motions generally conform to expectations based on previous studies. Forward-directivity motions may have larger displacement response in the long-period range than would be predicted by the equal-displacement rule. The strength-reduction factor,  $R$ , appropriate for forward-directivity motions may need to be reduced somewhat relative to other classes of motion if ductility demands are to be held constant.

The displacements of the Takeda oscillators were sometimes several-fold greater or less than those of the bilinear oscillators. Although it is fundamentally important to consider displacements in seismic response, variability of the response estimates as affected by ground motions and hysteresis model must also be considered.

Previous damage, modeled as prior ductility demand, did not generally cause large increases in displacement response when the Takeda models with positive post-yield stiffness were exposed to performance-level earthquakes associated with life safety or collapse prevention. Prior ductility demands were found to cause mean changes in displacement response ranging from  $-3\%$  to  $+10\%$  for the Takeda5 and TakPinch oscillators having no strength degradation (Figures 6-55 and 6-56). PDDs of 8 often caused a slight decrease in the displacement response computed using the Takeda5 and TakPinch models; response infrequently was 20% to 30% or more higher than that for the undamaged oscillator.

For oscillators having cyclic strength degradation, represented by the TakPinch oscillators, the effect of strength degradation was generally to increase the mean displacement response, but only by a few percent. The mean increase was larger for the structures having lower DDD, reaching as much as 21% for oscillators having  $RSR = 0.6$ . This result merely indicates that strength degradation tends to cause displacement response to increase relative to undamaged or nondegrading systems. Further examination revealed that increasing PDD increases or decreases the mean response of TakPinch systems with strength degradation by only a few percent (Figure 6-56). The weaker oscillators, represented by larger DDD, are more likely to exhibit damage in a real earthquake, and to have smaller increases in displacement due to prior ductility demands.

While prior damage causes relatively small changes in mean displacement response relative to undamaged structures, it also introduces some variability in displacement response. Variability in response is inherent in earthquake-resistant design, and the variability introduced by prior damage should be considered in the context of variability arising from different ground motions, choice of hysteretic models, modeling assumptions, and other sources. For example, Figures 6-32 to 6-34 illustrate the degree to which different earthquakes can cause bilinear and Takeda oscillators of equal strength to have substantially different peak displacement response. Thus, the variability in response introduced by prior damage is not considered significant.

Three NSPs for estimating peak displacement response were applied to the Takeda oscillators. Significant variability in the estimated displacements, when compared with the values calculated from nonlinear dynamic analysis, underscores the difficulty in accurately estimating response of a SDOF system to a known ground motion. The accuracy of the NSP estimates is compared in Figure 6-63. In Figure 6-64 it can be observed that the capacity spectrum and coefficient methods are more accurate, in a mean sense, than the secant method, and that all methods tend to overestimate the displacement response of short-period Takeda5 oscillators.

The NSPs were also used to estimate the change in displacement caused by a prior earthquake. Given the relatively small effect of damage on peak displacement response, it appears that damaged structures should be modeled similar to their undamaged counterparts, in order to obtain identical displacement estimates for performance events that are stronger than the damaging event. This results in damage having no effect on the displacement response, which closely approximates the analytical results.

The accuracy with which an NSP accounts for strength reduction was explored. It was found that each NSP was reasonably able to capture the effect of strength reduction.

The above findings pertain to systems characterized by ductile flexural response having degrading stiffness, with and without pinching. Systems with negative post-yield stiffness were prone to collapse, even with DDD of 2. Such systems should remain nearly elastic if their collapse is to be avoided.



## 6.8 References

- Araki, H., Shimazu, T., and Ohta, Kazuhiko, 1990, "On Residual Deformation of Structures after Earthquakes," *Proceedings of the Eighth Japan Earthquake Engineering Symposium—1990*, Tokyo, Vol. 2, pp. 1581-1586. (In Japanese with English abstract.)
- ATC, 1996, *Seismic Evaluation and Retrofit of Concrete Buildings*, Applied Technology Council, ATC-40 Report, Redwood City, California.
- ATC, 1997a, *NEHRP Guidelines for the Seismic Rehabilitation of Buildings*, prepared by the Applied Technology Council (ATC-33 project) for the Building Seismic Safety Council, published by the Federal Emergency Management Agency, Report No. FEMA 273, Washington, D.C.
- ATC, 1997b, *NEHRP Commentary on the Guidelines for the Seismic Rehabilitation of Buildings*, prepared by the Applied Technology Council (ATC-33 project) for the Building Seismic Safety Council, published by the Federal Emergency Management Agency, Report No. FEMA 274, Washington, D.C.
- Boroschek, R.L., 1991, *PCNSPEC Manual, (Draft)*, Earthquake Engineering Research Center, University of California at Berkeley.
- Cecen, H., 1979, *Response of Ten-Story Reinforced Concrete Model Frames to Simulated Earthquakes*, Doctoral Thesis, Department of Civil Engineering, University of Illinois at Urbana.
- Fajfar, P. and Fischinger, M., 1984, "Parametric Study of Inelastic Response to Some Earthquakes Recorded in Southern Europe," *Proceedings of the Eighth World Conference on Earthquake Engineering*, Vol. 4, pp. 75-82.
- Humar, J., 1980, "Effect of Stiffness Degradation on Seismic Response of Concrete Frames," *Proceedings of the Seventh World Conference on Earthquake Engineering*, Vol. 5, pp. 505-512.
- Iwan, W.D., 1973, "A Model for the Dynamic Analysis of Deteriorating Structures," *Proceedings of the Fifth World Conference on Earthquake Engineering*, Vol. 2., pp. 1782-1791.
- Iwan, W.D., 1977, "The Response of Simple Stiffness Degrading Systems," *Proceedings of the Sixth World Conference on Earthquake Engineering*, Vol. 2, pp. 1094-1099.
- Kawashima, K., Macrae, G., Hoshikuma, J., and Nagaya, K., 1994, "Residual Displacement Response Spectrum and its Application," *Journal of Structural Mechanics and Earthquake Engineering*, Japan Society of Civil Engineers, No. 501, pp. 183-192. (In Japanese with English abstract.)
- Lepage, A., 1997, *A Method for Drift Control in Earthquake-Resistant Design of RC Building Structures*, Doctoral Thesis, Department of Civil Engineering, University of Illinois at Urbana.
- Mahin, S.A., 1980, "Effects of Duration and After-shocks on Inelastic Design Earthquakes," *Proceedings of the Seventh World Conference on Earthquake Engineering*, Vol. 5, pp. 677-679.
- Mahin, S.A., and Lin, J., 1983, *Construction of Inelastic Response Spectra for Single-Degree-of-Freedom Systems—Computer Program and Applications*, Earthquake Engineering Research Center, University of California at Berkeley, Report No. UCB/EERC-83/17, Berkeley, California.
- Mahin, S.A., and Boroschek, R., 1991, *Influence of Geometric Nonlinearities on the Seismic Response and Design of Bridge Structures*, Background Report to California Department of Transportation, Sacramento, California.
- Minami, T., and Osawa, Y., 1988, "Elastic-Plastic Response Spectra for Different Hysteretic Rules," *Earthquake Engineering and Structural Dynamics*, Vol. 16, pp. 555-568.
- Miranda, E., 1991, *Seismic Evaluation and Upgrading of Existing Buildings*, Doctoral Thesis, Department of Civil Engineering, University of California, Berkeley.
- Moehle, J.P., Browning, J., Li, Y.R., and Lynn, A., 1997, "Performance Assessment for a Reinforced Concrete Frame Building," (abstract) *The Northridge Earthquake Research Conference*, California Universities for Research in Earthquake Engineering, Richmond, California.
- Nakamura, T., and Tanida, K., 1988, "Hysteresis Model of Restoring Force Characteristics of Reinforced Concrete Members," *Proceedings of the Ninth World Conference on Earthquake Engineering*, Paper 6-4-7, Vol. VI.
- Nasser, A.A., and H. Krawinkler, H., 1991, *Seismic Demands for SDOF and MDOF Systems*, John A. Blume Earthquake Engineering Center, Stanford University, Report No. 95, Stanford, California.

- Newmark, N.M., and Riddell, R., 1979, "A Statistical Study of Inelastic Response Spectra," *Proceedings of the Second U.S. National Conference on Earthquake Engineering*, pp. 495-504.
- Otani, S., 1981, "Hysteresis Models of Reinforced Concrete for Earthquake Response Analysis," *Journal (B)*, Faculty of Engineering, University of Tokyo, Vol. XXXVI, No. 2, pp. 125 - 159.
- Palazzo, B., and DeLuca, A., 1984, "Inelastic Spectra for Geometrical and Mechanical Deteriorating Oscillator," *Proceedings of the Eighth World Conference on Earthquake Engineering*, Volume IV, pp. 91-98.
- Parducci, A., and Mezzi, M., 1984, "Elasto-Plastic Response Spectra of Italian Earthquakes Taking into Account the Structural Decay," *Proceedings of the Eighth World Conference on Earthquake Engineering*, Volume IV, pp. 115-122.
- Paulay, T. and Priestley, M.J.N., 1992, *Reinforced Concrete and Masonry Buildings: Design for Seismic Resistance*, Wiley & Sons, New York.
- Qi, X., and Moehle, J.P., 1991, *Displacement Design Approach for Reinforced Concrete Structures Subjected to Earthquakes*, Earthquake Engineering Research Center, Report No. UCB/EERC 91/02, University of California at Berkeley, Berkeley, California.
- Rahnama, M., and Krawinkler, H., 1995, "Effects of P-Delta and Strength Deterioration on SDOF Strength Demands", *Proceedings of the 10<sup>th</sup> European Conference on Earthquake Engineering*, Vol. 2, pp. 1265-1270.
- Riddell, R., 1980, "Effect of Damping and Type of Material Nonlinearity on Earthquake Response," *Proceedings of the Seventh World Conference on Earthquake Engineering*, Vol. 4, pp. 427-433.
- Saïidi, M., 1980, "Influence of Hysteresis Models on Calculated Seismic Response of R/C Frames," *Proceedings of the Seventh World Conference on Earthquake Engineering*, Vol. 5, pp. 423-430.
- Sewell, R.T., 1992, "Effects of Duration on Structural Response Factors and on Ground Motion Damageability," *Proceedings of the SMIP92 Seminar on Seismological and Engineering Implications of Recent Strong Motion Data*, pp. 7-1 to 7-15.
- Shimazaki, K., and M.A. Sozen, M.A., 1984, *Seismic Drift of Reinforced Concrete Structures*, Research Reports, Hasama-Gumi Ltd., Tokyo (in Japanese), and draft research report (in English).
- Somerville, P.G., Smith, N.F., Graves, R.W. and Abrahamson, N.A., 1997, "Modification of Empirical Strong Ground Motion Attenuation Relations to Include the Amplitude and Duration Effects of Rupture Directivity," *Seismological Research Letters*, Vol. 68, No. 1.
- Takeda, T., Sozen, M.A., and Nielsen, N.N., 1970, "Reinforced Concrete Response to Simulated Earthquakes," *Journal of the Structural Division*, American Society of Civil Engineers, Vol. 96, No. ST12, pp. 2557-2573.
- Wolschlag, C., 1993, *Experimental Investigation of the Response of R/C Structural Walls Subjected to Static and Dynamic Loading*, Doctoral Thesis, Department of Civil Engineering, University of Illinois at Urbana.
- Xie, L.-L., and Zhang, X., 1988, "Engineering Duration of Strong Motion and its Effects on Seismic Damage," *Proceedings of the Ninth World Conference on Earthquake Engineering*, Vol. 2, Paper 3-2-7.

# 7. Example Application

## 7.1 Introduction

This section gives an example of the use of FEMA 306 recommendations to evaluate earthquake damage in a two-story reinforced-concrete building. The example is meant to be as realistic as possible and is based on an actual structure.

### 7.1.1 Objectives

The example is intended to help evaluating engineers understand such issues as:

- the overall process of a FEMA 306 evaluation.
- accounting for pre-existing damage.
- how both observation and analysis are used in the evaluation procedures.
- determining and using the applicable FEMA 306 Component Damage Classification Guides, including cases where an exactly applicable damage guide is not provided.
- foundation rocking of walls, which may be a prevalent behavior mode in many structures.
- some of the ways engineering judgment may need to be applied.
- how restoration measures can be determined based on either the *direct method* or the *performance analysis method*.
- aspects of using a nonlinear static procedure of analysis (pushover analysis).
- establishing displacement capacities and demands.

Reading through the example could be the best introduction to an understanding of the FEMA 306 evaluation process. References to the applicable sections of FEMA 306 or 307 (or to other sources) are given in “bookmark” boxes adjacent to the text. Because the example is meant to be illustrative, it contains more description and explanation than would normally be contained in an engineer’s evaluation report for an earthquake-damaged building.

It should be clear from this example that the FEMA 306 recommendations for evaluating earthquake damage

must be implemented under the direction of a knowledgeable structural engineer, particularly when a performance analysis is carried out. The responsible engineer should have a thorough understanding of the principles behind the FEMA 306 recommendations and should be familiar with the applicable earthquake research and post-earthquake field observations. FEMA 307 provides tabular bibliographies and additional information on applicable research.

A fundamental tenet of the component evaluation methods presented in FEMA 306 is that the severity of damage in a structural component may not be determined without understanding the governing behavior mode of the component, and that the governing behavior mode is a function not only of the component’s properties, but of its relationship and interaction with surrounding components in a structural element. In the following sections, the evaluation of the example building emphasizes the importance of this principle. There may be a temptation among users of FEMA 306 to use the damage classification guides as simple graphical keys to damage, and to complete the analysis by simply matching the pictures in the guides to the observed damage. The example is intended to show that this is not the appropriate use of the guides. It is organized to emphasize the importance of the analytical and observation verification process that is an essential element of the evaluation procedure.

### 7.1.2 Organization

The example is organized as shown in the flow chart of Figure 7-1. This organization follows the overall evaluation procedure outlined in FEMA 306, beginning with a building description and observations of earthquake damage.

The building has been subjected to a previous earthquake. The damage investigation establishes the pre-existing conditions so that the loss from the recent earthquake can be evaluated. The preliminary classification of component types, behavior modes, and damage severity are made by observing the structure. It is shown, however, that classification of behavior modes, and hence damage severity, may be unclear when based on observation alone. Simple analytical tools provided in the material chapters of FEMA 306 are used to verify the expected component types and behavior modes, and damage severity is assigned accordingly. The steps required to estimate the loss by the direct method are

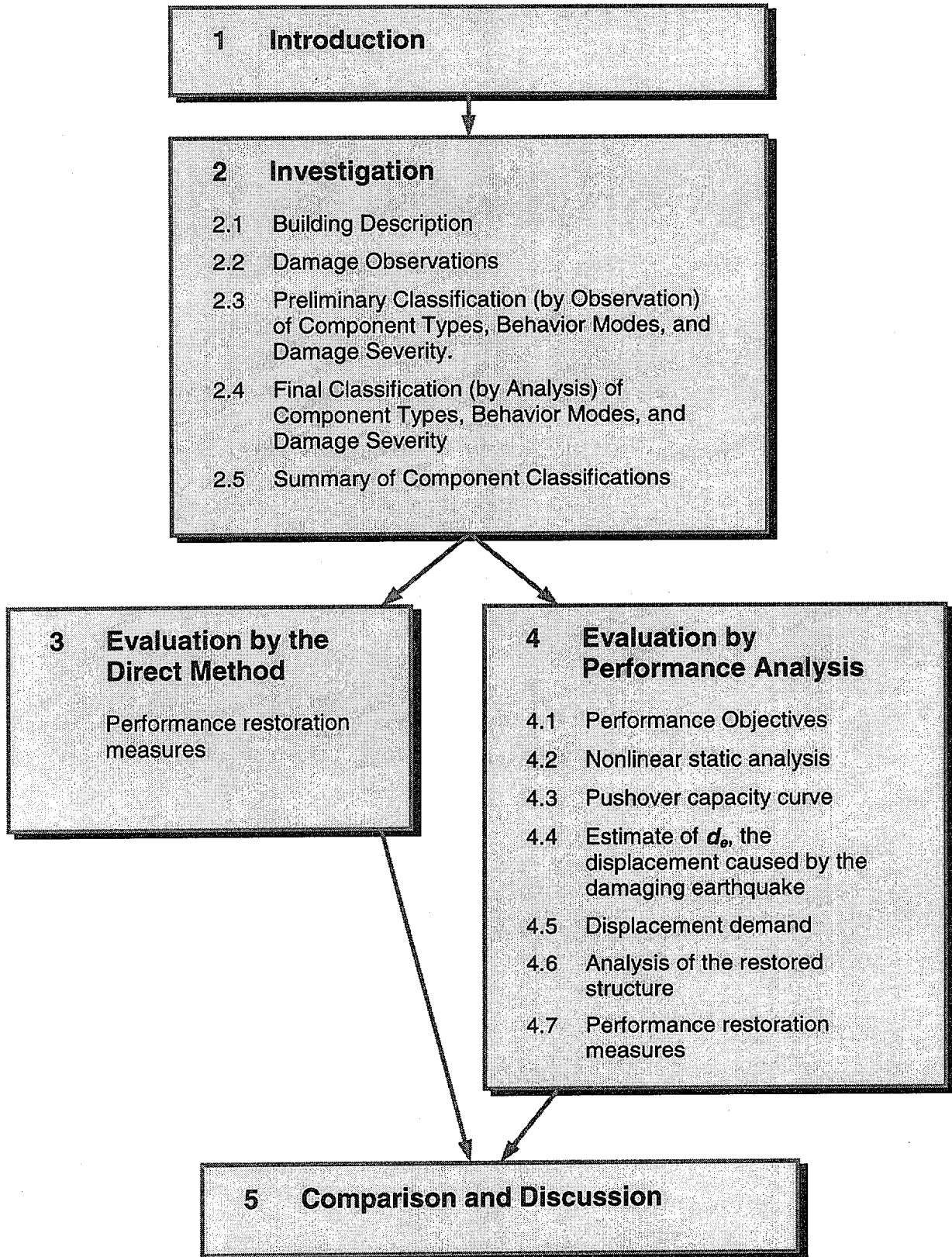


Figure 7-1 Flowchart for example

illustrated, and a relative performance analysis is carried out. It is emphasized that the direct method provides only loss estimation information, and that a relative performance analysis is required in order to make performance-based design decisions.

Damage records for all of the structural walls of the building are included. The damage records for two of the walls are discussed in detail. Damage records for the remaining walls are given at the end of the example.

## 7.2 Investigation

### 7.2.1 Building Description

The example building is a two-story concrete building located on a sloping site. The building is a “T” shape in plan with the stem of the T on the downhill side, containing a partial lower story below the other two stories. The building was designed and constructed in the late 1950s. The building is located about 3.6 miles from the epicenter of the damaging earthquake.

The overall plan dimensions of the building are 362 feet in the North-South direction by 299 feet in the East-West direction. The floor slabs cantilever about 6 feet from the perimeter columns forming exterior sun-screens/balconies. The building facade along the perimeter is set back 8 feet from the edge of the slab. For the typical floor, the interior floor area is about 62,600 square feet, and the total slab area is about 70,400 square feet. The lower level encompasses about 20,200 square feet. Floor plans are shown in Figure 7-2 and an elevation is shown in Figure 7-3. The roof of the building supports mechanical equipment.

The floors and roof are constructed with waffle slabs comprised of a 4-½ inch thick slab and 14 inch deep pans (18-½ inches total depth). Columns supporting the slabs are typically spaced at 26 feet in each direction. The interior columns are 18-inch square and the perimeter columns are 18-inch diameter. The columns are supported on spread footings.

Reinforced concrete walls in both directions of the building resist lateral forces. The walls are 12 inches thick and are cast monolithically at each end with the gravity-load-carrying columns. The walls are typically located along corridors, and the corridor side of the wall has a 1-inch thick plaster coat. The typical solid wall configuration and reinforcement are shown in Figure 7-4.

In the lower level there are several reinforced concrete masonry (CMU) walls that are framed between the ground and the first floor slab (basement level) in the three-story section of the building. The CMU walls are attached to the first floor slab. However, these walls were not designed as shear-resisting elements. Because the first floor slab is anchored to the foundation in the two-story portion of the building, the contribution of the CMU walls to the lateral force resistance, particularly in the east-west direction, is minimal.

Several of the reinforced concrete walls have door openings, 7 feet 3 inches tall by 6 feet 6 inches wide, in the middle of the wall, creating a coupled wall. The typical coupled wall configuration and reinforcement are shown in Figure 7-5. In the three-story section of the building (the stem of the T), the walls are discontinued at the lower level. This lower level contains a single reinforced concrete wall in the north-south direction centered between the two walls above.

### 7.2.2 Post-earthquake Damage Observations

Following the damaging earthquake, the engineers performed a post-earthquake evaluation of the building. The initial survey was conducted one month after the damaging earthquake. The structural drawings for the building were reviewed. The follow-up investigations were conducted about three months following the earthquake.

Visual observation, Guide NDE1, Section 3.8 of FEMA 306

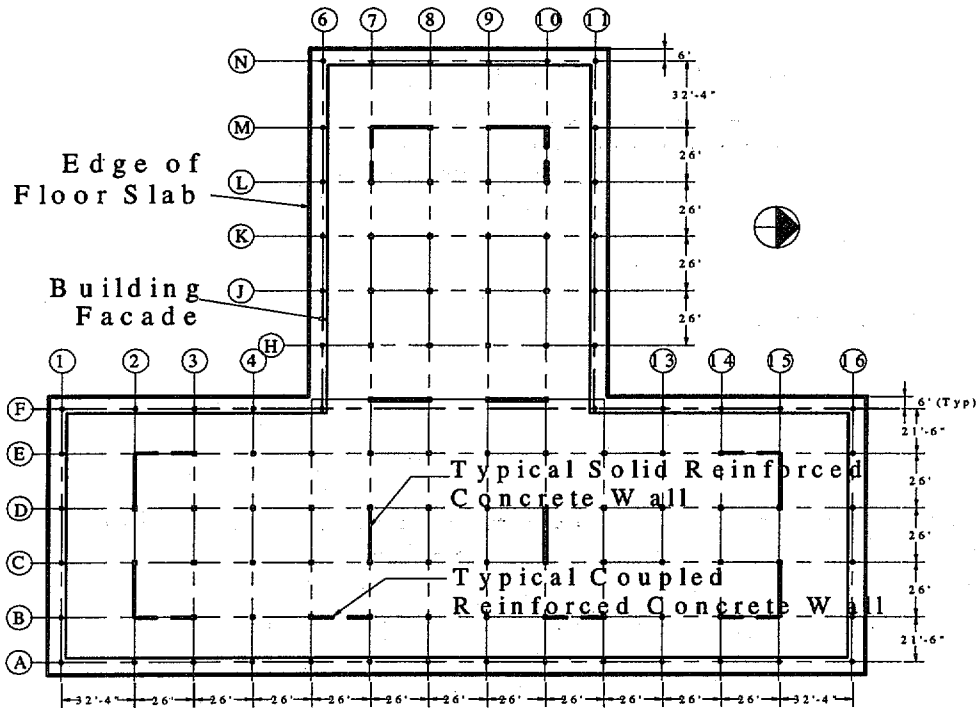
The post-earthquake evaluations were conducted using visual observation techniques on exposed surfaces of the structural elements. The sections of wall above the ceiling were typically observed only where the suspended ceiling tiles had fallen during the earthquake. Crack widths were measured at selected locations using magnifying crack comparators for most of the significant cracks in each wall.

#### 7.2.2.1 Pre-Earthquake Conditions

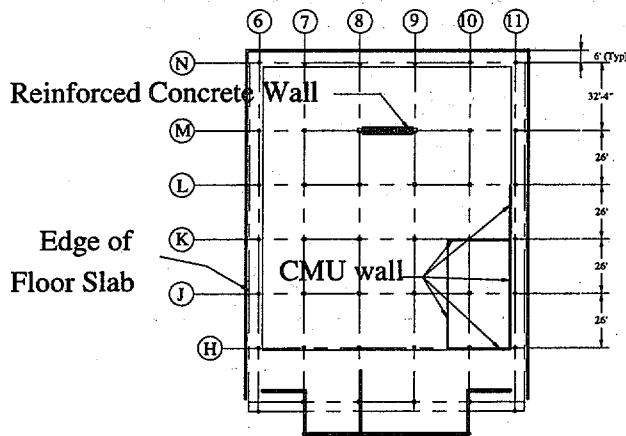
The building had experienced some cracking prior to the damaging earthquake. The pre-existing damage is judged to have been caused by a previous earthquake. The heaviest damage appeared to have been in the coupling beams. The wall cracks above the ceiling line were observed to have been repaired by epoxy injection.

Old cracks vs. new cracks, Section 3.4 of FEMA 306

## Chapter 7: Example Application



a) First and Second Floor Plan



b) Basement Floor Plan

Figure 7-2 Floor Plans

## Chapter 7: Example Application

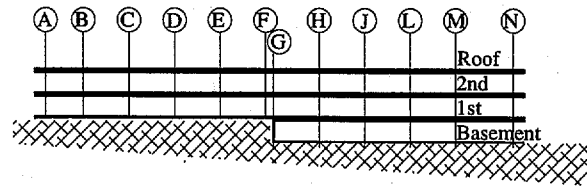


Figure 7-3 Building Cross-section

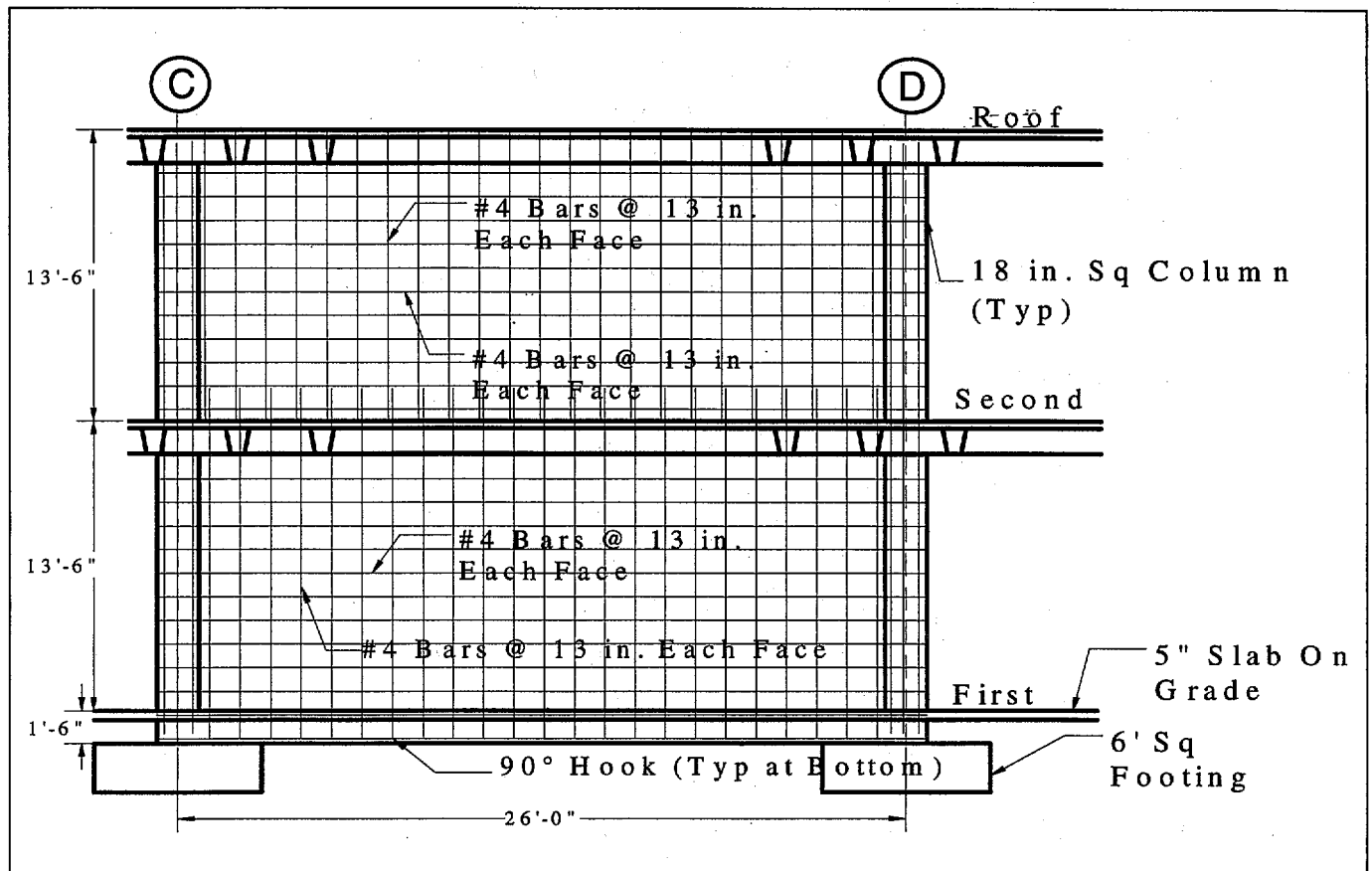


Figure 7-4 Example Solid Wall Detail (Condition at Line 7)

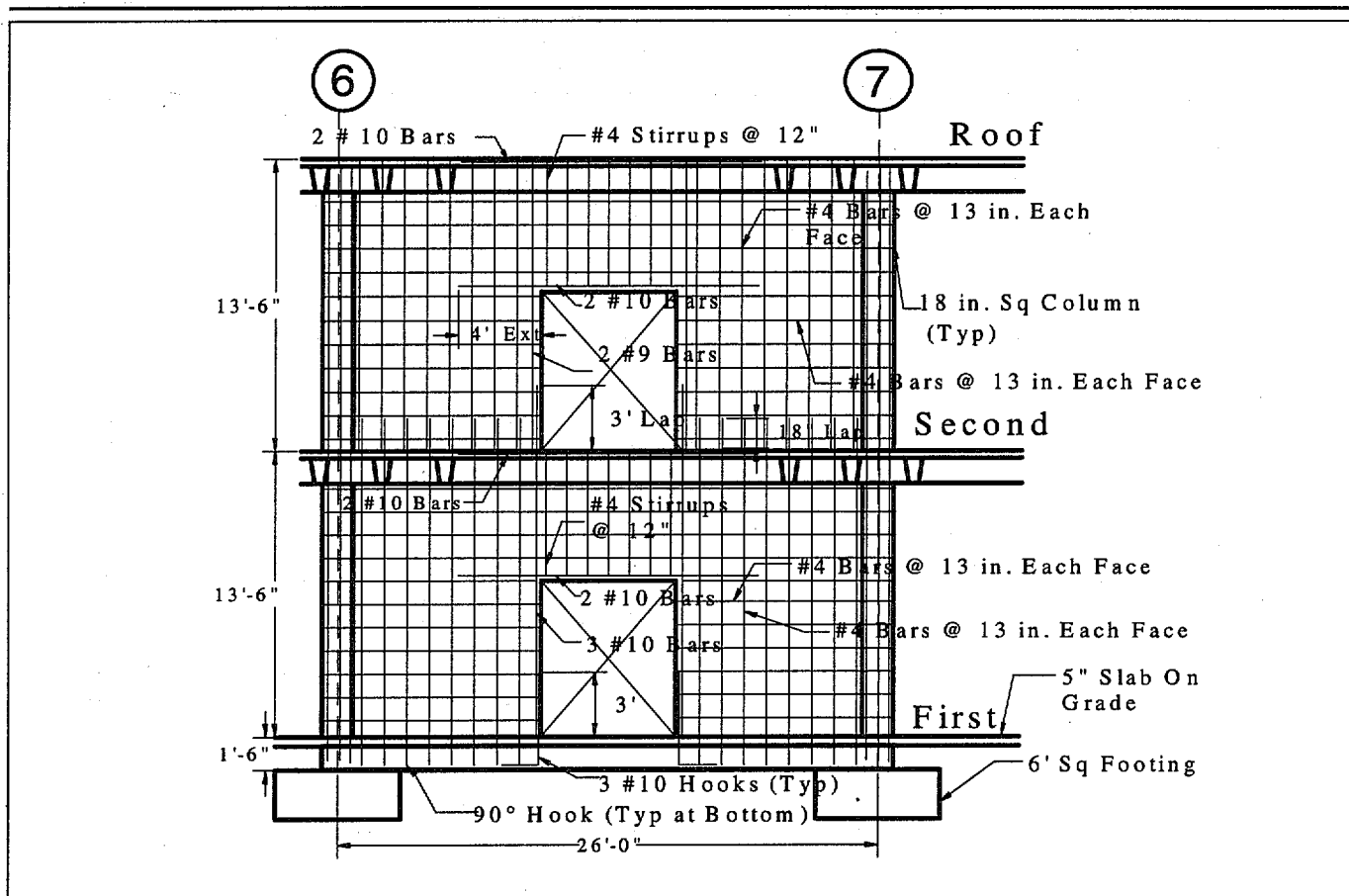


Figure 7-5 Example Coupled Wall Detail (Condition at line B)

Below the ceiling the cracks may also have been injected with epoxy. However, the architectural finishes on those surfaces obscured the evidence of the previous repairs. Many of the cracks in the plaster coat on the walls appeared to have been cosmetically repaired using a strip of fabric and plaster placed over the crack. It was not clear whether the underlying cracks in the concrete had been repaired. Therefore, the building is assumed to have some cracking prior to the damaging earthquake and the pre-existing cracking is taken into account by reducing the pre-event stiffness of the concrete walls.

#### 7.2.2.2 Postearthquake Condition and Damage Documentation

The concrete walls experienced minor to moderate amounts of cracking. Based on the visual observations, component damage records were prepared for each of the walls in the building. These forms are included as Figures 7-6, 7-7, and in Appendix A, Component Damage Records D1 through

Documentation of damage, Section 3.7 of FEMA 306

D19. Each of the component damage records depicts the observations for both stories of a two-story wall, except for the single-story wall on the lower level shown on Record D19. All observable cracks are shown, but only those cracks found to be wider than 30 mils (1/32 inch) have the crack width, in mils, written on the component damage record at the approximate location of the measurement. Cracks found to be previously repaired with epoxy and those with pre-existing surface patches are indicated. Spalls are also noted.

The two first-story coupled walls in the stem of the T section of the building experienced heavy cracking in the coupling beams (Column lines 7 and 10, L to M, Component Damage Records D4 and D6). One of the other coupling beams (Column Line B, 14 to 15, Record D12) also experienced heavy cracking. The damage to the coupling beams included some spalling of the concrete, buckling of reinforcing bars, and cracking of the floor slab adjacent to the wall. Several walls were



Figure 7-6

Solid Wall Example

Element / Component Damage Record		
<b>Building Name:</b> Concrete Shear Wall Building	<b>Project ID:</b> ATC 43 Example	<b>Prepared by:</b> ATC
<b>Location Within Building:</b> Floor: 1 <sup>st</sup> /2nd      Column Line: 2		<b>Date Inspected:</b> 24-Sep-97
Sketch and Description of Component and Damage:		
<b>Legend:</b> Crack (Width < 0.030 inch) Crack Width in Mills (0.001 Inch) Crack Previously Filled with Epoxy Crack at Pre-existing Surface Patch Spall Not Accessible Partition Key Plan		

PRELIMINARY CLASSIFICATION  
BY OBSERVATION

COMPONENT TYPE
RC1

BEHAVIOR MODE
B,C,H or M

DAMAGE SEVERITY
Moderate if H Insignificant if B,C, or M

FINAL CLASSIFICATION  
BY ANALYSIS

COMPONENT TYPE
RC1

BEHAVIOR MODE
M (Overturning)

DAMAGE SEVERITY
Insignificant

Figure 7-7

Coupled Wall Example

Element / Component Damage Record		
Building Name: Concrete Shear Wall Building	Project ID: ATC 43 Example	Prepared by: ATC
Location Within Building: Floor: 1 <sup>st</sup> /2nd      Column Line: 7		Date Inspected: 24-Sep-97
Sketch and Description of Component and Damage:		
<div style="display: flex; justify-content: space-around; align-items: center;"> <div style="text-align: center;"> <p>(L)</p> </div> <div style="text-align: center;"> <p>(M)</p> </div> </div>		
<p><b>Legend:</b></p> <div style="display: flex; justify-content: space-between;"> <div style="width: 45%;"> <p> Crack (Width &lt; 0.030 inch)</p> <p> Crack Width in Mills (0.001 inch)</p> <p> Crack Previously Filled with Epoxy</p> <p> Crack at Pre-existing Surface Patch</p> </div> <div style="width: 45%;"> <p> Spall</p> <p> Not Accessible</p> <p> Partition</p> </div> </div> <div style="text-align: center; margin-top: 10px;"> <p>Key Plan</p> </div>		

**PRELIMINARY CLASSIFICATION  
BY OBSERVATION**

COMPONENT TYPE		
	RC3	
RC1	RC3	RC1

BEHAVIOR MODE		
	B or H	
N	B or H	N
B, C, H, or	B or H	B, C, H, or

DAMAGE SEVERITY		
	Insig. or Moderate	
Insignificant or Moderate	Heavy	Insignificant or Moderate

**FINAL CLASSIFICATION  
BY ANALYSIS**

COMPONENT TYPE		
	RC3	
RC1	RC3	RC1

BEHAVIOR MODE		
	H	
N	H	N

DAMAGE SEVERITY		
	Moderate	
Insignificant	Heavy	Insignificant